Summer 2021

Advancements In Bio-based Novel (co)Monomers for Polymeric Materials

Khristal Anne Monroe

ADVANCEMENTS IN BIO-BASED NOVEL (co)MONOMERS FOR POLYMERIC MATERIALS

by

KHRISTAL ANNE DELABAR-MONROE

(Under the Direction of Rafael L. Quirino)

ABSTRACT

Most current research in the area of sustainable and environmentally friendly materials relate to the use of renewable sources for the fabrication of bio-based polymers and composites. Using plant-based derivatives is a common strategy. Pine sap can be distilled into turpentines (light fraction) and pine rosin (heavy fraction). Pine rosin is obtained as a brittle solid and its major component is abietic acid. This project aims at investigating a synthetic approach for the synthesis of a pine rosin-based polymer that can be potentially used for manufacturing a collection device for pine sap. The synthetic strategy consisted in the preparation of tung oil abietate in two steps. The first step leads to tung oil diglyceride from the transesterification of tung oil with glycerol. Confirmation of the formulated tung oil diglyceride was given by analyzing the compound with Fourier Transmission Infrared and Raman Spectroscopy, Gas Chromatography, Nuclear Magnetic Resonance analysis, Thermal Gravimetric Analysis and Differential Scanning Calorimetry analysis. The second step converts tung oil diglyceride into tung oil abietate via an acid-catalyzed esterification with pine rosin. Confirmation of the tung oil abietate went through Fourier Transmission Infrared and Raman Spectroscopy, Nuclear Magnetic Resonance analysis, Thermal Gravimetric Analysis and Differential Scanning Calorimetry analysis. By developing a monomer that combined the two compounds, it was believed that pine rosin could be developed into a functional polymer. The approach investigated involves the bulk free radical co-polymerization of pine rosin with *n*-butyl methacrylate and divinylbenzene. Di-*tert*-butyl peroxide was used as the free radical initiator. Through observation alone the tung oil abietate polymer appeared almost black and hard to the touch. Using a thermal analysis to confirm formation of the polymer, the Thermal Gravimetric Analyzer and Differential Scanning Calorimetry

instruments were used. Both instruments gave positive results that the polymer was cured completely using 140 ℃ at an 18hr interval.

INDEX WORDS: Bio-derived, Bio-based materials, Pine rosin, Abietic acid, Carboxylic acid, Transesterification, Esterification, Free-radical polymerization, Polymerization, Monomer, Polymer

ADVANCEMENTS IN BIO-DERIVED NOVEL (co)MONOMERS FOR POLYMERIC MATERIALS

by

KHRISTAL ANNE DELABAR-MONROE

B.S., Georgia Southern University, 2018

A Thesis Submitted to the Graduate Faculty of Georgia Southern University in

Partial Fulfillment of the Requirements for the Degree

MASTER OF SCIENCE

ADVANCEMENTS IN BIO-DERIVED NOVEL (co)MONOMERS FOR POLYMERIC MATERIALS

by

KHRISTAL ANNE DELABAR-MONROE

Major Professor:	Rafael Quirino
Committee:	Shainaz Landge
	Ji Wu

Electronic Version Approved:
July 2021

DEDICATION

Looking back, I have far more supporters than I probably deserve. To keep it simple, I dedicate this to my son, Ezekiel L. Monroe. He encompasses all that I am grateful for as well as all the motivation to finish.

ACKNOWLEDGMENTS

First, I must recognize my entire team and community of family in the Chemistry and Biochemistry Department of Georgia Southern University.

Dr. Shainaz Landge, you are more than just my advisor, you are a friend that has shown me when I need to change and hold myself accountable and to a higher standard. You have given me so much more than knowledge of the craft. Dr. Debajana Ghosh, you changed my world in more ways than just teaching me General Chemistry II, thank you. Dr. Ji Wu, thank you for making me think about my data on a deeper level. I need to be more confident in myself as well as assured of my answers. Dr. Nate Takas, you became a dear friend. We share the like in knowledge, and you put up with my weirdness and oddities. Thank you for believing in me. Thank you Dr. McGibony for putting up with my crazy freak out moments and supporting me through all of them.

My entire graduate team of friends!! MARIA BLAHOVE!!! Ricardo Belloso, Hunter Whitetree, Nadia Singleton

Thank you Dr. Quirino for believing in me after I met you for the first time in 2016. Rafa, you mean more to me than you will ever understand. You kept me true to myself. You dealt with all my crazy antics and quick judgements. You gave me the time to learn more than just chemistry. Thank you for the immeasurable patience and love that you gave as a mentor and an advisor.

And last, my family. When I stop to put them on paper, it amazes me how many more there are than I truly take the time to realize. There would be no way to give all my reasons of thanks, but for true acknowledgement here are their names: Rose and Carl Delabar, Joshua A. Monroe, Ezekiel L. Monroe, Carl Joseph and Michelle Delabar, Helen Martinson, Carl Benard and Joyce Delabar, Rebecca M. Shipwash-Villegas (Go Eagles!), Jessica Parfait, Carrie Beasley, Tonya Haynes-Blake, Kendra Adams (and Donnie!),

TABLE OF CONTENTS

LIST OF TABLES

Page

LIST OF FIGURES

Page

LIST OF SCHEMES

Page

THESIS ORGANIZATION

The thesis is organized into four chapters. The first chapter introduces heavy support for bio-based and bio-derived polymers that encompass pathways to better materials for the future. Introduction consists of a thorough review of literature that supports bio-materials focusing on vegetable oil derivatives. Chapter two revolves around the choice of pine rosin (>80% abietic acid) as the beginning base that grew into forming a novel monomer with tung oil for this thesis. The methodology that develops the carboxylic acid within the pine rosin (>80% abietic acid) into a monomer with tung oil is supported with the characterization analysis. This flows into chapter three with early polymerization production of the novel monomer that consists of preliminary characterization of the ten different tung oil abietate samples. The polymerization proceeds via a free radical process. The fourth chapter concludes the thesis by stating how the tung oil abietate polymer will need further investigation. Future work for the polymer is vital for composite development.

CHAPTER 1

INTRODUCTION

It is not possible to stop employing crude oil for petrochemical products. However, it is still a necessity to reduce crude oil usage. Even if the crude oil market has become economically sound currently causing easier access to manufacture petrochemical products, there is a trend over time that portrays that it is not always financially reliable[1]. Petrochemical usage from fossil fuels is not sustainable nor is the unnatural release of stored carbon good for Earth.[1,2,3] There are new developments that help chemical industry to utilize mechanical infrastructure already in place to produce bio-based compounds which makes this alternative a more viable option.[1,3,4] Unlike the century of evolution for crude oil-based products, the bio-based alternatives have quickly developed within a twenty-to-thirty-year period. To encourage these alternatives there has been more support from the social front causing a small amount of legislative change initiating the use of bio-based products.[1,4] The whirlwind of the 21st century has driven the support for government programs like *BioPreferred* that seek out bio-derived remedies.[1] With this in mind, the challenges ahead entangle harnessing how to employ, the finances to produce and the performance of bio-based materials.[1]

Product research with renewable resources is not novel. Research studies that work with some form of plant derived compound have been occurring for decades as the need for renewable resources becomes more abundantly clear with the need to maintain Earth.[1,4] Early on bio-based research relied heavily on plant compounds from first generation feedstocks which is a raw material that come from edible plant sources like corn and potato. Both of these crops are rich in carbohydrate material monomers making it a great renewable source. However, using first generation feedstock for chemical products is trumped by the use of these crops for human and animal consumption.[1,5] This leads to employing second generation feedstocks such as wood byproducts like pulp and non-edible oils and resins.[1,5] Second generation sources are not suitable for consumption and the agricultural waste can be used in research for bio-based polymer composites and bio-based thermosets.[1,5] All of these are rich with bio-based material, but research is met

with the issue of processing first and second generation bio-based material.[1,5] There is leading research in the third and fourth generation feedstocks for sources of biomass type fuels. Third generation is algae based and is quickly becoming a front runner for fuels and polymer research due to its rich oil content.[5] Fourth generation is relatively new and sourced through plant engineering process that allows for carbon capture and storage technique.[5]

Are there possible reactions and techniques that can reduce material processes that alleviates research barriers for non-edible plant sources? Industry also meets new research with a wall of questions about the equipment and tools needed to extract and manufacture these bio-based compounds.[1] Present day chemical industry infrastructure is mostly designed for distillation and fractionation. To upfront the cost to either refurbish present-day infrastructure, replace or procure building sites solely for processing the bio-based compounds is a hefty investment.[1,3] Processing the bio-based material involves heavy amounts of energy put in just to use for either energy production or material manufactured products[1], but, as stated above, this is rapidly changing due to a good trend change and push for research with alternative bio-based polymers.[5] Pyrolysis methods by anaerobic conditions are one of those trend changes. Using pyrolysis to decompose biomass byproducts such as lignin and kernel shells produces bio-oil that can be fractionated into viable compounds such as carboxylic acids.[4,5,6,7] Choi et al. has used a fast pyrolysis bed reactor and in **figure 1** is a blueprint that would allow industry to employ infrastructure already in place. True distillation is the purification of liquid material, but many chemical companies use pyrolysis since this heating method can fractionate from a solid.[1,3]

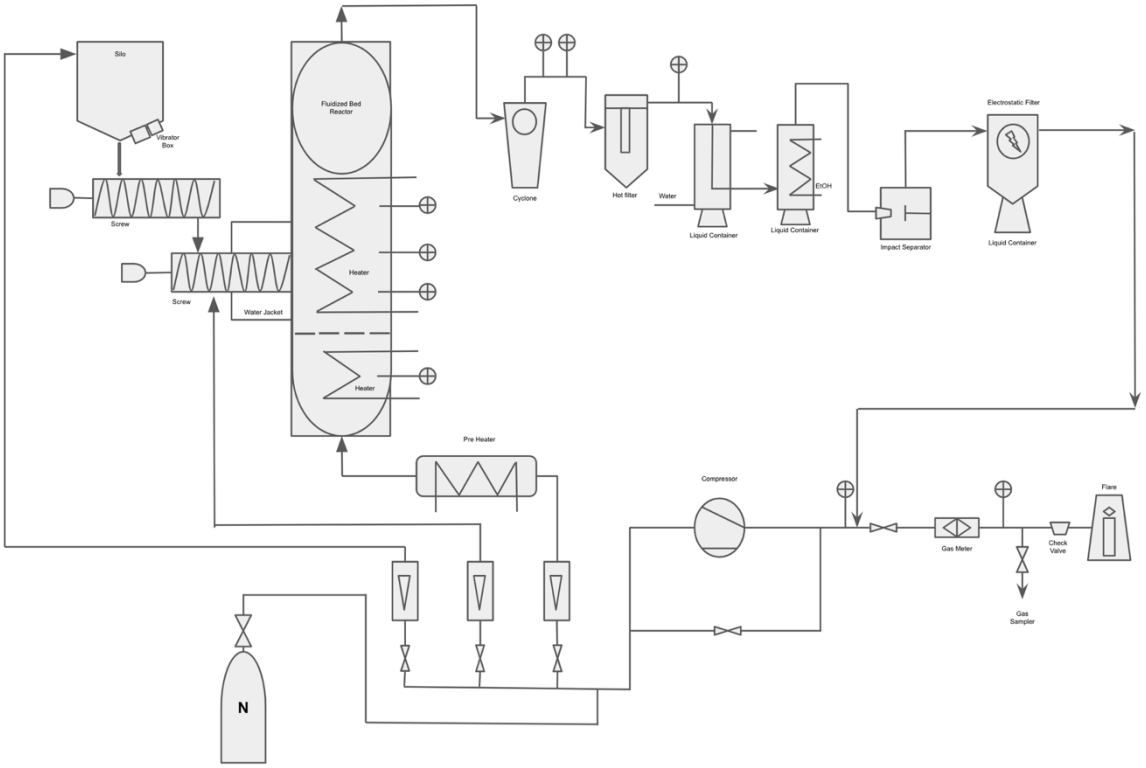

Figure 1: Diagram of the fast pyrolysis process using a feeding system that separates into a fluidized-bed reactor, char separation system, quenching system, impact separator and electrostatic precipitator, and gas catch circulator.

It would be good to note that there is a difference in terminology when describing bio-based polymers. There are bio-based polymers and biodegradable polymers. Simply put, biodegradable polymers are a subset of bio-based polymers defined by the polymers thermo-type.[1,8] Plant compounds are being sought for monomers that mimic the latest properties in petrochemical based thermoset and thermoplastic products.[1,2,3,7,8] Thermosets are heavily crosslinked through intermolecular covalent bonding and do not recycle very well.[1] Thermosets are more purposed for long term use within commercial business and residential household usage and building materials.[1] Thermoplastics, on the other hand, consist of independent polymer chains held together through non-covalent interactions, making it easier to break down for recycled plastics and biodegradability.[1]

That is where pine rosin comes into this research approach. Pine rosin is the hard brittle by-product of the heavy fraction from distilled pine resin harvested from *Pinus elliottii* and other pine species.[8,9] This pine species is well known as Slash Pine which is a non-food crop grown in Georgia and throughout the southeastern United States making it more desirable being a local regional accessible material.[8,9]

The experimental approach is to take pine rosin and manipulate it into a bio-based polymer and composite for an alternative to petrochemical based products. The compound being explored within pine rosin is abietic acid (AA). AA is a natural terpene with a tricyclic phenanthrene ring structure, including two conjugated double bonds and functional groups, such as a carboxylic acid (**Figure 2**).[9,10] Pine rosin (>80% abietic acid) is explored in many areas already for its functionality since it is so easily epoxidized and oxidized. The world's production of pine rosin and its terpenoid resin acids is ~1.2 million tons annually.[4,9,11] Pine rosin (>80% abietic acid) can be extracted from either distillation or pyrolysis giving it yet another quality as a promising bio-renewable compound.[7]

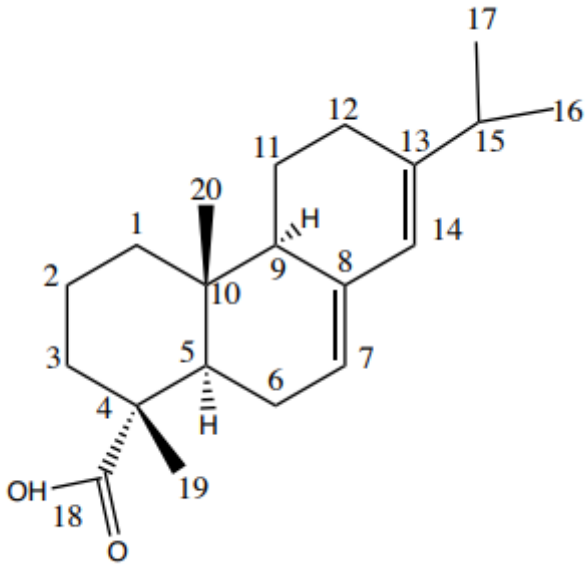

Figure 2: Chemical structure of abietic acid within pine rosin.

Bio-based polymers are most notably constructed with vegetable oils.[1,2,3] Popularity for vegetable oils grew out of the vast availability that began from its start in first generation feedstock research.[1,2,5] This stems from the rich triglycerides found in vegetable oils. Triglycerides contain useful fatty acid chains such as linolenic acid, **α**-eleostearic (**Figure 3**) and oleic acid.[7,8] **Figure 3** is the triglyceride found in tung oil with a composition of >80% **α**-eleostearic (18:3). Oleic acid is a monounsaturated fatty acid found in Olive oil.[8] Linseed oil contains linolenic acid that has unconjugated fatty acid chains.[7,8] Fatty acids are not all the same and their composition is contingent on plant type, environment and geographical location.[8]

Seen in **figure 3** the fatty acid found in tung oil has three specific conjugated C=C bonds located at the 9(cis), 11(trans) and 13(trans) carbons.[8] These three C=C bonds do not need modification to polymerize unlike many other vegetable oils. Tung oil can readily polymerize through cationic, free radical or thermal polymerization.[8] This specific triglyceride offers great functions in polymer and material chemistry due to its reactivity from conjugation.[8]

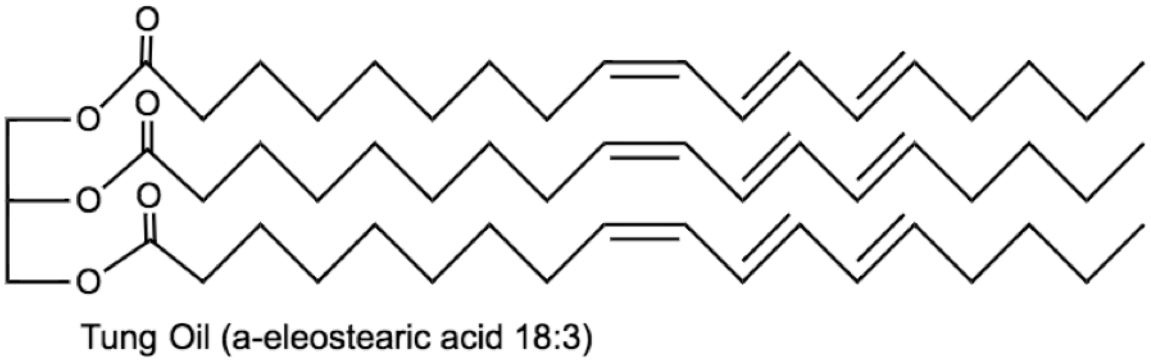

Figure 3: Chemical structure of tung oil.

This study proposes a new approach toward a renewable sustainable product with pine rosin (>80% abietic acid) in whole for structural applications. The existing products that contain monomers from pine rosin are mainly epoxy resins used in industry for construction applications, such as flooring, adhesives,

and coatings.[11] The exploration of literature has found that the use of pine rosin has been modified prior to experimentation for new approaches toward polymerizing abietic acid such as Ganewetta et al. using dehydroabietic acid. However, Hasan et al. used a purchased 85% abietic acid mixture of naturally occurring components and isomerized the abietic acid afterwards during the reaction for a liquid crystalline epoxy. This research is constructing a polymer from the bulk whole of pine rosin without isolating a specific molecule to manipulate.

Initial attempts to carry out a direct free radical polymerization of pine rosin (>80% abietic acid), without the addition of any co-monomers, were unsuccessful. Likewise, the direct free radical polymerization of turpentine was unsuccessful. In an attempt to obtain a reactive monomer from pine rosin (>80% abietic acid), a synthetic strategy was employed for the preparation of tung oil abietate (**Scheme 1**). Combining tung oil and pine rosin (>80% abietic acid) as a single monomer allows the free radical polymerization triggered by peroxide initiators, as performed previously.[8] Tung oil (>80% **α**-eleostearic acid) is a triglyceride with an unsaturated triple conjugation fatty acid composition.[8] Being able to use two non-food crop plant-based compounds together that molecularly enhance each other can allow a stable starting point to provide great material to form a polymer. Free radical polymerization is easily done through a heat cure that belays the need for any extra solvent curing. This type of reaction supports greener alternatives and less waste accumulation.

CHAPTER 2
PINE ROSIN AND TUNG OIL

Abietic Acid (AA) corresponds to over 80% of the diterpene resin acids in pine rosin.[9,12,13] Work currently being pursued within Quirino's lab indicates the viability of pine rosin (>80% abietic acid) to construct a workable monomer. Pine rosin (>80% abietic acid) is currently used in the preparation of emulsions, inks, adhesives, and coatings.[4,11] It has recently taken on new avenues within biofuels due to its oxidation properties related to the conjugated carbon-carbon double bonds of the terpene system which can be seen in **figure 2**.[4,9,13,16] That same conjugated system can potentially work favorably towards free radical reactions, following the same concept explored in the free radical polymerization of conjugated vegetable oils.[8] Vegetable oils like tung oil that have conjugation have proven valuable in bio-based polymers. Tung oil has had great results as a biopolymer and a monomer within a comonomer polymerized as a crosslinked thermoset.[8]

In preliminary trials, the bulk free radical polymerization of pine rosin alone did not result in a viable polymer, prompting the chemical modification of pine rosin (>80% abietic acid) into a more reactive bio-based monomer. Since tung oil has shown significant promise as a co-monomer for the preparation of bio-based thermosets, a synthetic strategy was proposed for the preparation of tung oil abietate (TOA) using the tung oil triglyceride and pine rosin (>80% abietic acid) (**Scheme 1**). Significant reactivity is expected for the proposed monomer since both tung oil and pine rosin possess conjugated carbon-carbon double bonds.

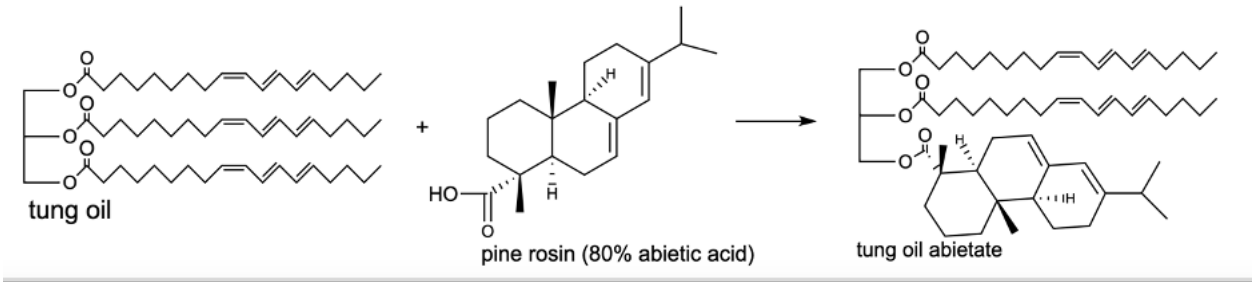

Scheme 1: Diagram of general idea to synthesize tung oil abietate using tung oil and pine rosin.

2.1 Materials

Pine Rosin was graciously donated by Diamond G Forest Product (Patterson, GA). Tung oil and 50% (w/w) sodium hydroxide solution were purchased from Sigma-Aldrich (St. Louis, MO). Glycerol was procured from Fisher Scientific (Fair Lawn, NJ).

2.2 Characterization

Fourier Transmission Infrared Spectroscopy (FTIR) was performed on the Thermo-Fisher Nicolet Avatar 370-FTIR (Waltham, MA). Raman spectroscopy was performed on the DXR Raman (Thermo Scientific, Waltham, MA). Thermal Gravimetric Analysis (TGA) tests took place using the TA Instruments Q50 thermogravimetric analyzer (New Castle, DE). All samples performed with the TGA were approximately 10 mg. They were measured for their thermal properties through a function of temperature with an atmosphere of air from 21 ℃ to 600 ℃ at a rate of 10 ℃/min. Differential scanning calorimetry was performed on a TA Instruments Q100 DSC equipped with a cooling unit (New Castle, DE) that scanned approximately 10 mg samples under a nitrogen atmosphere with a heating schedule of 20℃/min from 20℃ to 200 ℃. Gas Chromatography with Flame Ionization Detection (GC-FID) data collection was performed on a Shimadzu GC-2014 (Kyoto, Japan) and GC-Mass Spectrometry (GC-MS) data acquisition was performed on a Shimadzu GCMS-QP2010S with dual flow control and FID secondary detection (Kyoto, Japan). Methanol was used to prepare the sample. For the GC-FID/MS parameters a method was adapted

from literature from McGuire and Powis. Helium was the carrier gas used with 27.5 cm/s as the average linear velocity volume, the oven temperature at 150 ℃ and a split ratio of 100:1. The program consisted of an initial hold at 150 ℃ for ten minutes with a 5 ℃/min increase till 250 ℃ and holding at 250 ℃ for twenty minutes. The inlet injection and detector temperature were both 250 ℃. The mass spectrometer setting for the interface temperature was set to 280 ℃ and 70eV. The Agilent MR400DD2 NMR spectrometer (Santa Clara, CA) was used to acquire proton and carbon nuclear magnetic resonance at 400MHz.

2.2.1 Fourier Transmission Infrared and Raman Spectroscopy

Prior to the development of the novel monomer, instrumental characterization of pine rosin was utilized to determine its functional viability. The analysis of pine rosin was done with an ATR accessory attachment connected to the FTIR. **Figure 2** is a model structure of the main diterpenoid, abietic acid in pine rosin. This structure portrays the carboxylic acid located at carbon eighteen and the conjugation in the second and third ring. Seen in **figure 4** there is no true broad peak between 3500 cm^{-1} to 3000 that would represent the presence of the hydroxyl group in the carboxylic acid. However, due to the dimerization that occurs in pine rosin, the "OH" peak shifts into 2938 cm^{-1} C(*sp3*)-H absorption stretch.[12,13] Instead of this peak being large and sharp, it is broader and more medium. The C=O stretch in the carboxylic acid found at 1697 cm^{-1} is the most prominent peak in the spectrum.[12,13]

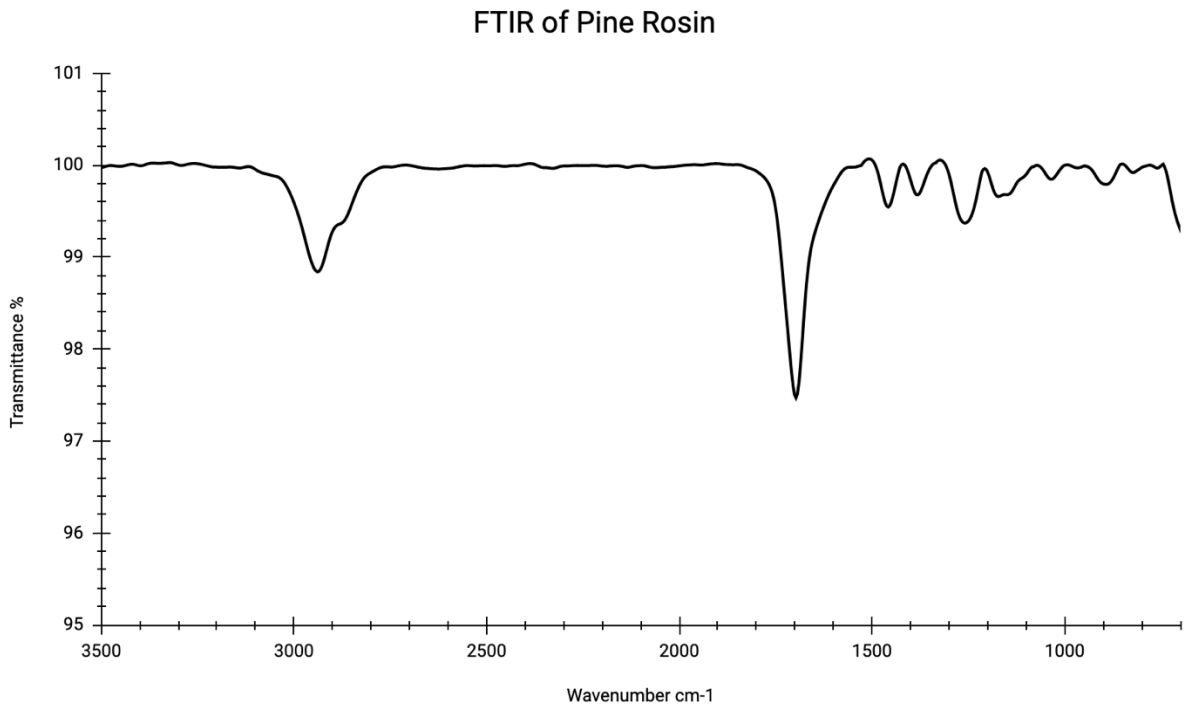

Figure 4: Fourier Transmission Infrared Spectrum of pine rosin (>80% abietic acid).

Raman spectroscopy compliments the findings obtained with FTIR spectroscopy by measuring any dipole moments the compound may have. While it may not be a prominent peak in **figure 4**, the Raman peak found at 1654cm^{-1} in **figure** 5 corresponds to the conjugated C=C bonds in the structure of pine rosin.[12,13] The other peaks are arbitrary.

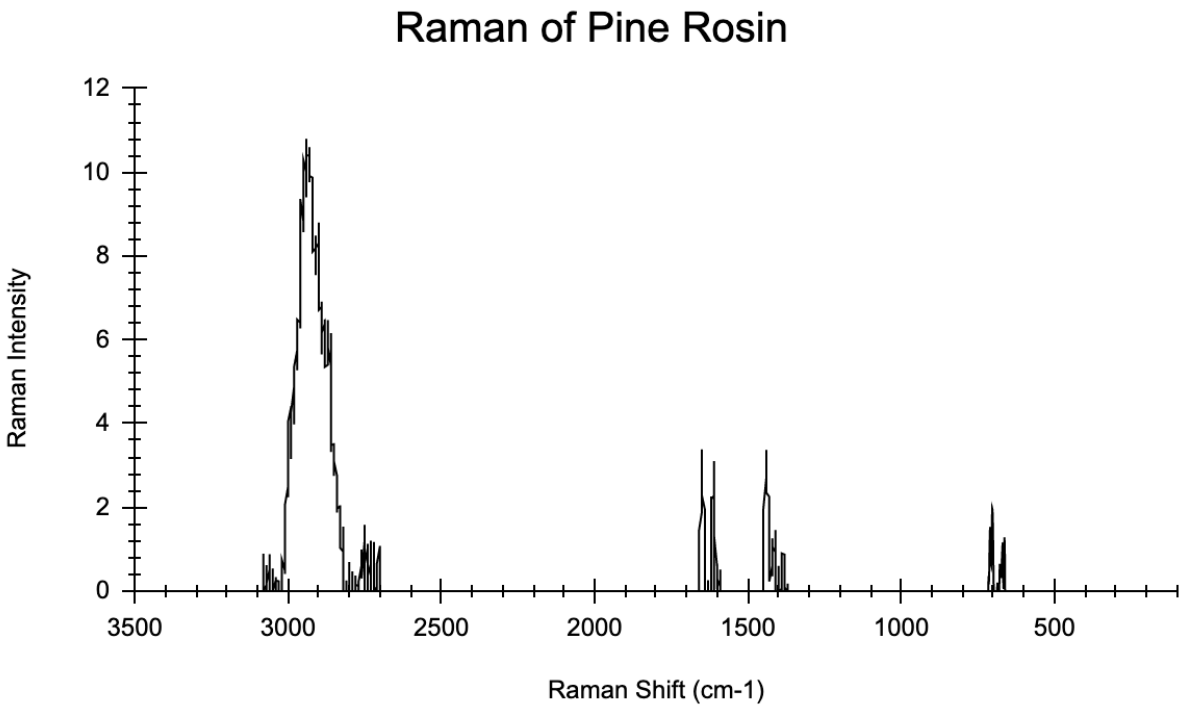

Figure 5: Raman Spectrum of pine rosin (>80% abietic acid).

2.2.2 Thermal Gravimetric Analysis

The thermal properties of pine rosin (>80% abietic acid) were assessed by TGA under a constant heating rate. In **figure 6,** the measurement of pine rosin indicates a pure substance due to major degradation occurring between 220 ℃ and 240 ℃. Even though pine rosin did not polymerize alone, the high degradation point was a step in the right direction. Thus, the thermal degradation point above 220 ℃ was great support for the proposed synthetic strategy to incorporate pine rosin.

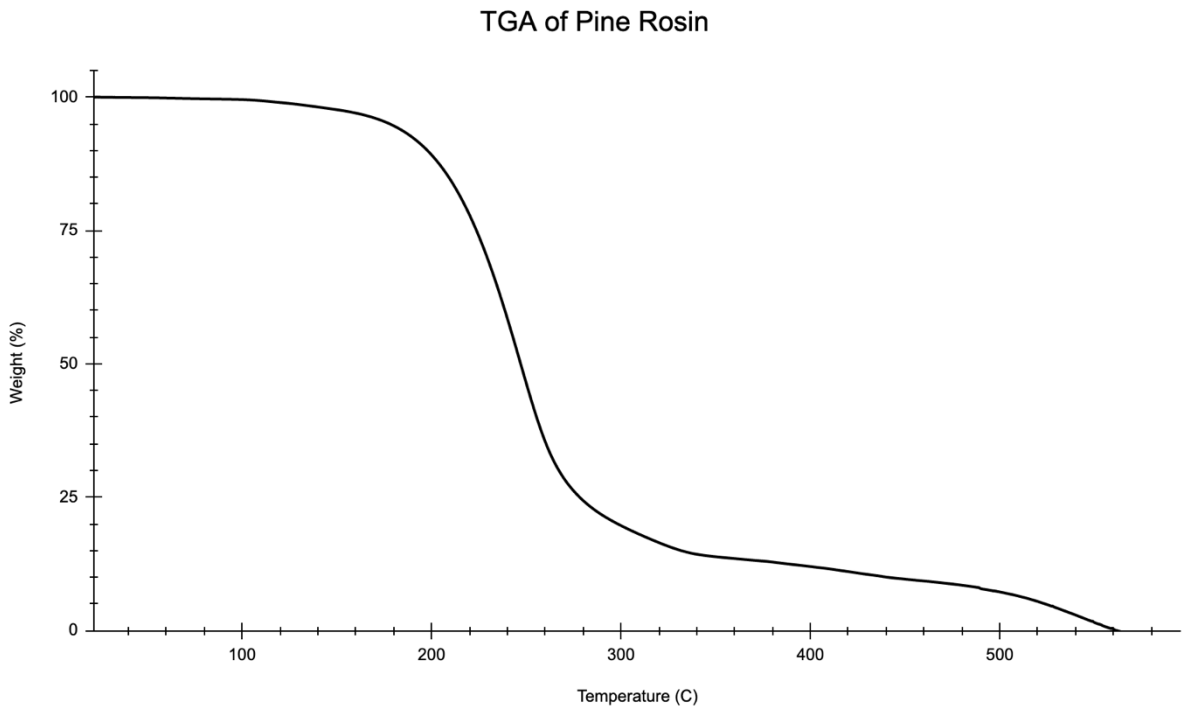

Figure 6: Thermal Gravimetric Analysis graph of pine rosin (>80% abietic acid).

2.2.3 Differential Scanning Calorimetry

Differential scanning calorimetry (DSC) is a common thermal analysis technique measuring heat flow exchange between a sample pan and reference pan through a constant heating rate. DSC was used to assess any significant thermal physical changes, such as crystallization or melting. Following thermogravimetric analysis, 200 ℃ was the max temperature chosen for DSC due to no degradation observed prior to that temperature with the TGA. In **figure 7**, a heat-cool-heat cycle is shown. There appears to be some questionable heating area during the first heating cycle of pine rosin., The TGA analysis was smooth in comparison. Since the two peaks are quite broad and follow each other in the same heating cycle between approximately 35 ℃ and 160 ℃, it is assumed there was heat flow exchange occurring. To support the prior statement, the second heating cycle appears much smoother with no true phase changes. A clear crystallization peak could not be detected upon cooling, indicating the lack

of crystallinity and therefore the amorphous state of solid pine rosin.[12,13] This analysis follows pine rosin's (>80% abietic acid) known melting point at 175 ℃ and boiling point at 250 ℃.[14]

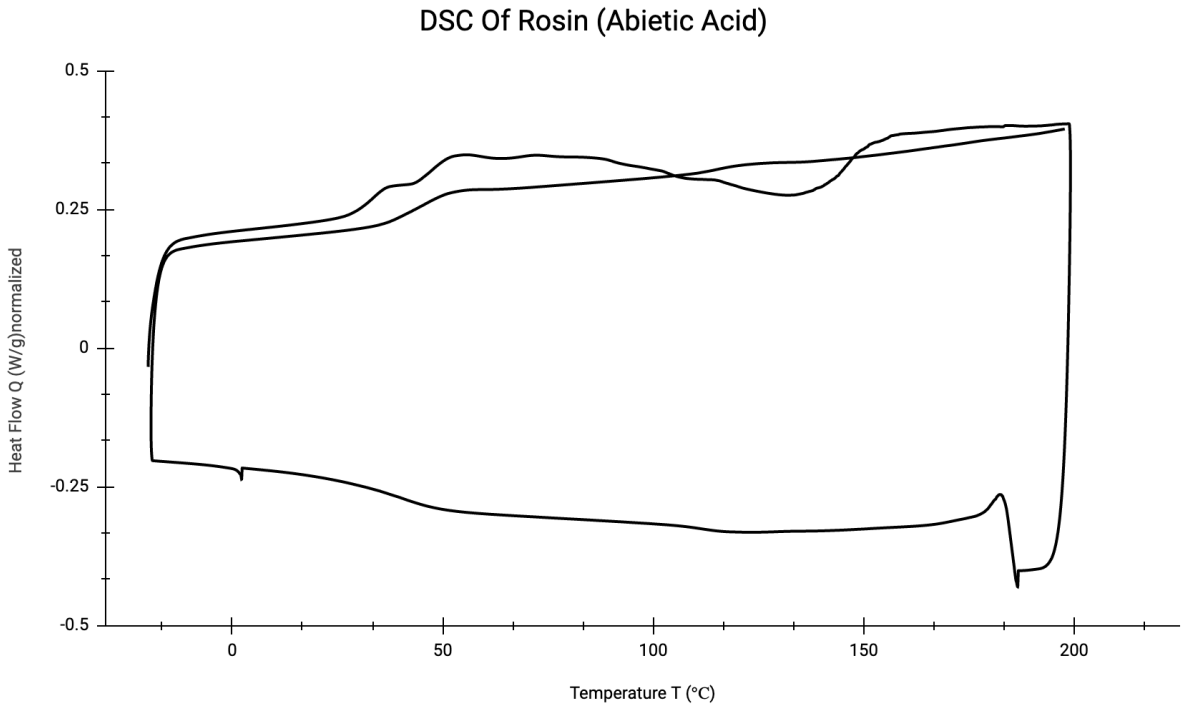

Figure 7: Differential Scanning Calorimetry graph of pine rosin (>80% abietic acid).

2.2.4 Gas Chromatography Flame Ionization Detection and Mass Spectroscopy

Pine rosin's boiling point is at 250 ℃.[11,14] The parameters for the GC measurement were setup with pine rosin's boiling point.[11,14] There was a sample measured on two different gas chromatography instruments, one equipped for flame ionization detection and the other with mass spectroscopy. However, the sample was made from straight pine rosin. Due to that factor and there was no specific molecule derivatized and/or isolated from pine rosin, the spectrum received in GCFID and GC-MS was too convoluted with all the molecules that make up the composition of pine rosin to truly recognize pine rosin as a pure substance on the GC spectrum (**Figure 8**).

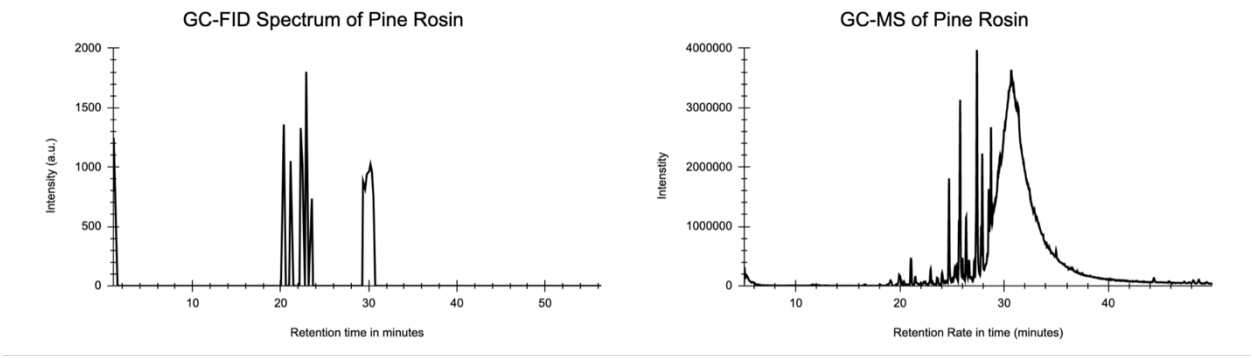

Figure 8: Gas Chromatography with Flame Ionization Detection and Mass Spectroscopy chromatogram of pine rosin.

2.2.5 Nuclear Magnetic Resonance

The ^{13}C (C) and ^{1}H (D) NMR spectrums in **figure 9** are enhanced for specific peaks. The carbon spectrum in **figure 9C** was enhanced to target the tallest singlet located at 184 ppm to identify the carboxylic acid in pine rosin.[15] **Figure 9B** represents the proton spectrum enhanced to target the singlet ~10.3 ppm that represents the carboxylic acid as well.[15]

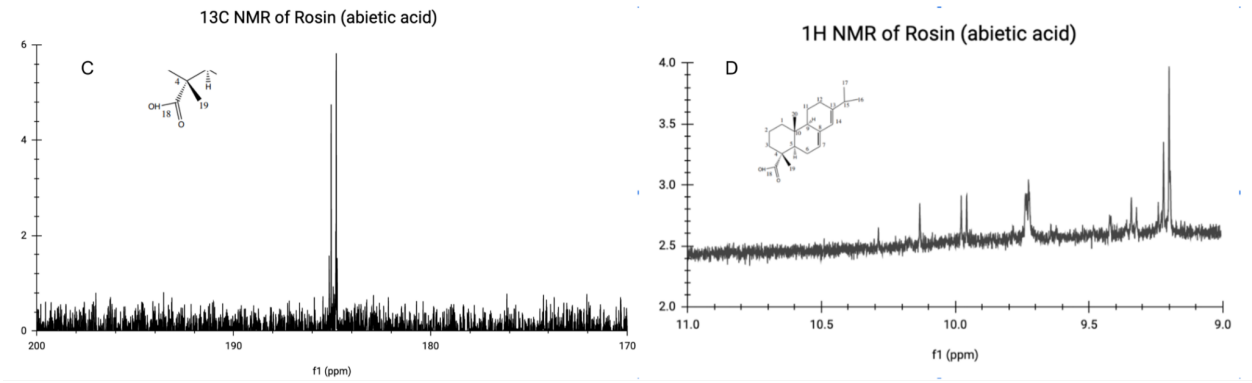

Figure 9: Nuclear Magnetic Resonance spectrums of ^{13}C (C) and ^{1}H (D) to show the presence of the carboxylic acid in pine rosin (>80% abietic acid).

2.2.6 Fourier Transmission Infrared and Raman Spectroscopy

For **figure 10** of the FTIR spectrum there are two peaks that stand out for tung oil. These are similar peaks to the ones that are found in pine rosin spectrum of FTIR analysis. These specifics peaks are the C(sp^3)-H at ~2920 cm^{-1} and an ester/carbonyl peak at 1745 cm^{-1}.[8] The first peak mentioned occurs from the alkane stretch vibrations.[8] The second peak that represents the carbonyl comes from the C-O stretch in the ester of the triglyceride.[8]

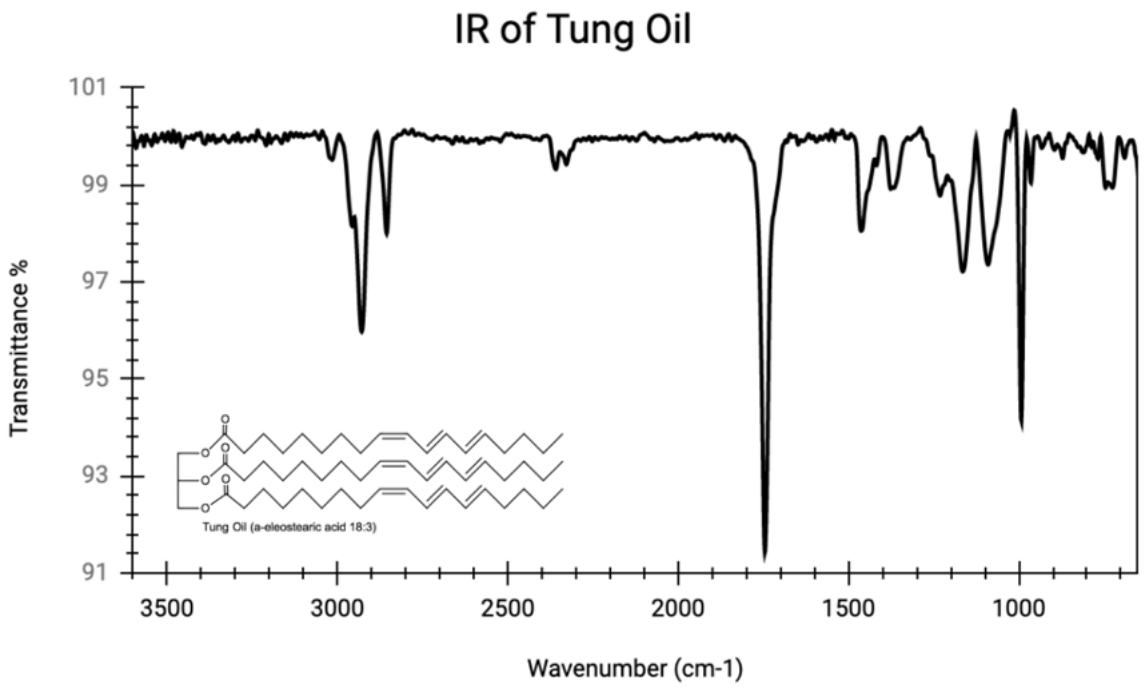

Figure 10: Fourier Transmission Infrared Spectrum of Tung oil.

Once again in the Raman spectrum for tung oil has an outstanding peak at 1640 cm^{-1} (**Figure 11**). This peak represents the dipole occurrence with conjugation located on the fatty acid chains of tung oil. Pine rosin has the same peak in its Raman analysis seen in **figure 5**. The difference between the two would be the intensity in tung oil is greater because of heavier conjugation.

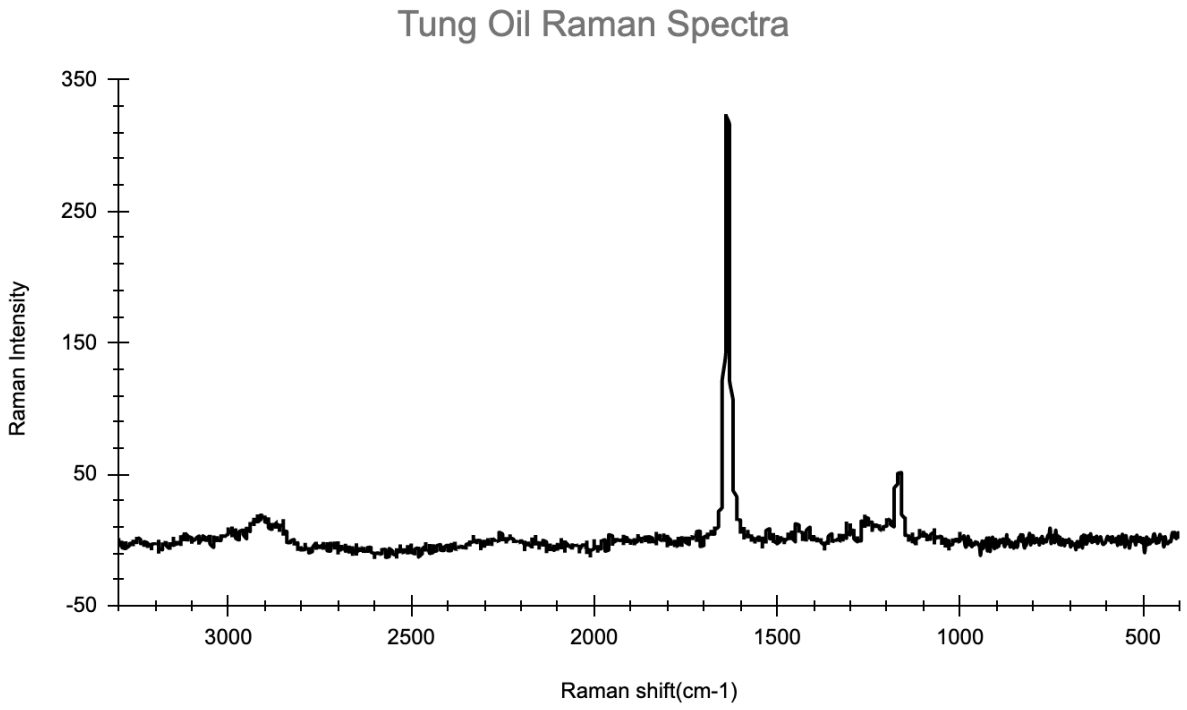

Figure 11: Raman Spectra of Tung Oil.

2.2.7 Thermal Gravimetric Analysis

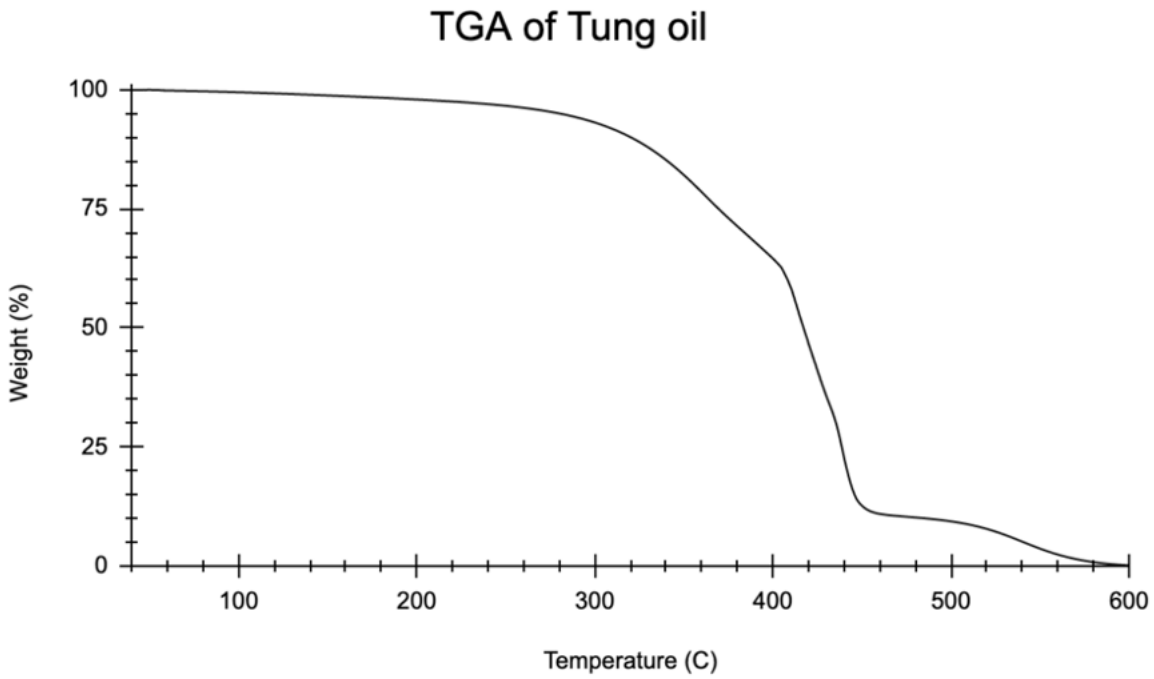

Figure 12: Thermal Gravimetric analysis of tung oil for its thermal properties using the Texas Instruments Q50 TGA.

Depicted in **figure 12** is the thermal gravimetric analysis of tung oil. This graph provided the thermal degradation point of tung oil at 320 ℃. The high degradation point of tung oil proposes good thermal stability. A thermal property such as this should in theory strengthen the synthesized monomer, tung oil abietate.

2.2.8 Differential Scanning Calorimetry

Following the TGA testing, a tung oil sample was measured for further thermal stability using DSC. There were no significant exothermic or endothermic spikes once again following the consistency of the thermal stability enhancement that tung oil should provide. Portrayed in **figure 13**, there was a phase change that occurred in the first heating cycle ~110 ℃ but does not cause concern because the cooling cycle and second heating cycle have no disruptions. The phase change is likely due to a heat flow exchange between the pans to equilibrate. This is a measurement to characterize thermal properties in tung

oil as a starting material to be used in the synthesized tung oil abietate and will be used to compare future measurements with DSC for tung oil abietate and its polymerization.

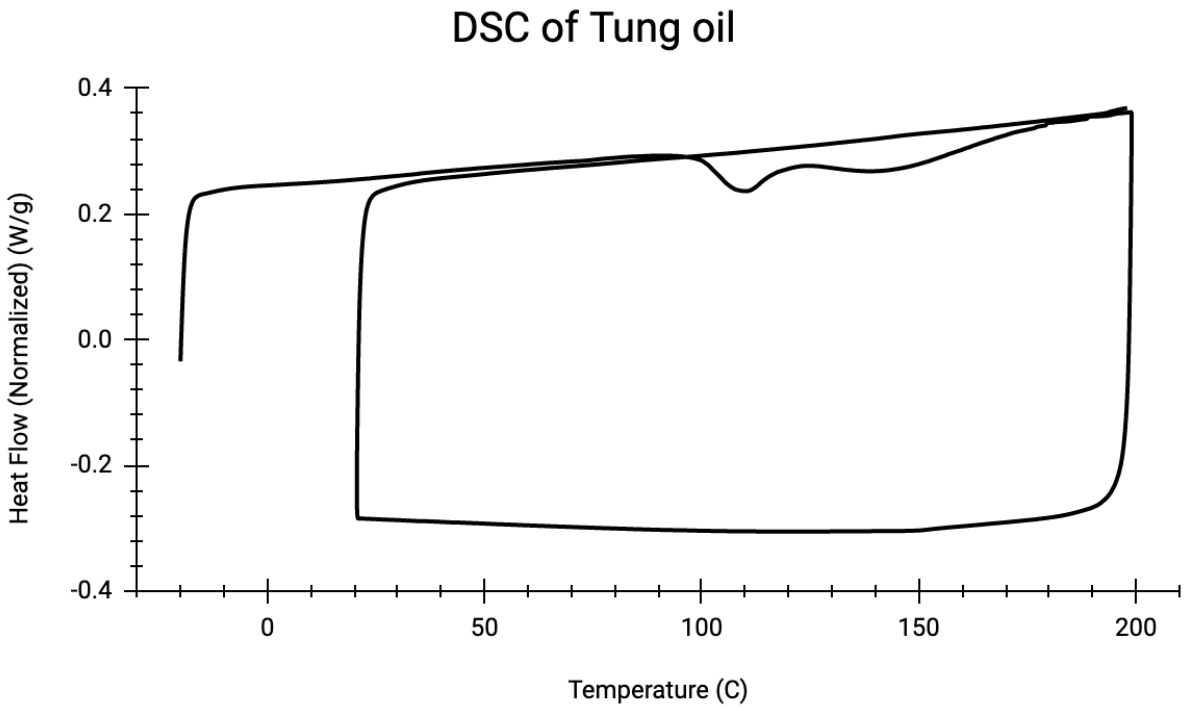

Figure 13: Differential Scanning Calorimetry analysis of Tung Oil.

2.2.9 Gas Chromatography Flame Ionization Detection and Mass Spectroscopy

GCFID/MS was used to characterize tung oil for its purity the same as pine rosin. Unfortunately, the same condition came into play with tung oil that occurred with pine rosin. The tung oil was not derivatized, purified or isolated for a specific molecule in its composition. This caused inconclusive spectrum data. There is also a large ghost peak that could be due to large clumping of the triglyceride being pushed out of the column **(Figure 14)**. After reflection of the characterization data in TGA, it was realized that tung oil boils ~>300 °C. The column parameters for this run were not hot enough for the instrument to properly elute such a large molecule.

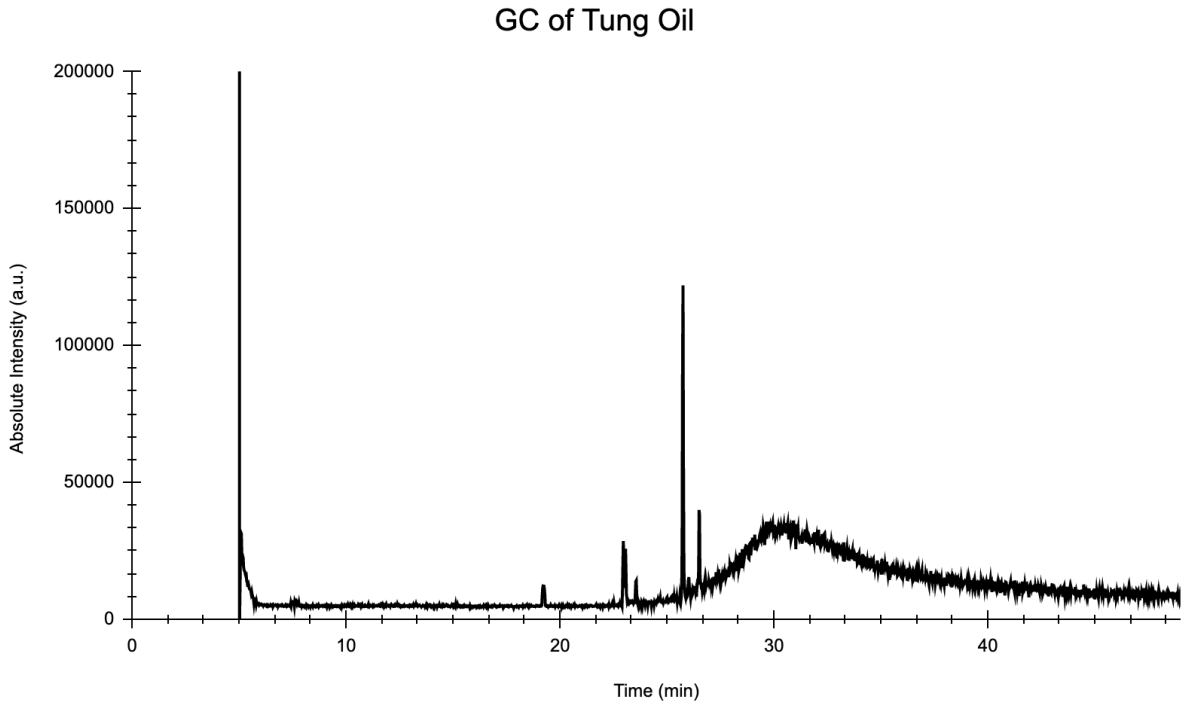

Figure 14: Gas Chromatography Flame Ionization Detection-Mass Spec spectrum of tung oil.

2.2.10 Nuclear Magnetic Resonance

The solvent used for this NMR was acetone. **Figure 15**, unlike the NMR spectrum for pine rosin, the ^{1}H proton spectrum was not enhanced to target specific peaks. The reference peak for the solvent is the largest peak at 2.08 ppm. To help with placement, tung oil is a triglyceride with more than eighty percent composition from **α**-eleostearic acid that is conjugated at carbons 9,11 and 13. The multiplets that occur at 4.2 ppm and 4.35 ppm support the glycerol backbone with the ester connection.[8,15] There is a triplet at 5.25 for the hydrocarbon backbone of the entire triglyceride.[8,15] There is a collection of multiplet peaks that occur from 5.40 ppm to 6.45 ppm due to conjugation and resonant effects on the **α**-eleostearic acid chains.[8,15]

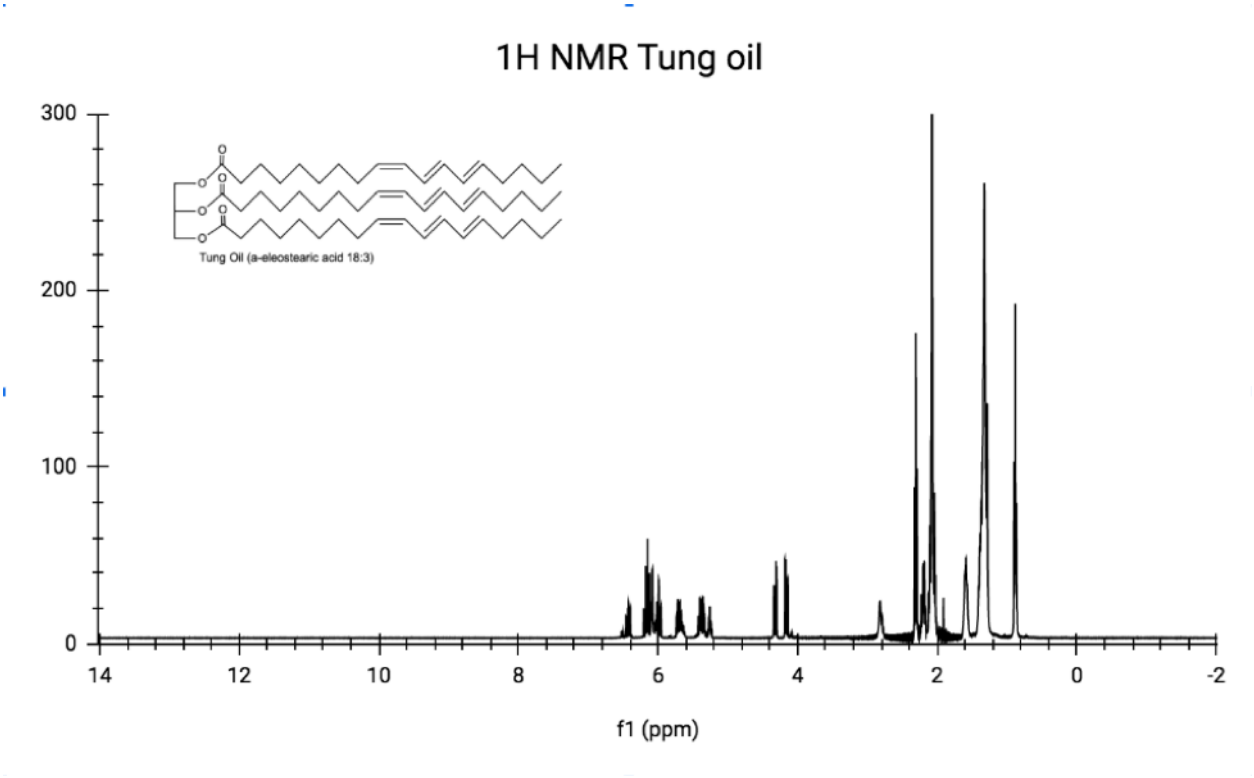

Figure 15: Nuclear Magnetic Resonance spectrums of ^{1}H spectra of Tung Oil.

2.3 Transesterification Reaction for the Modification of Tung Oil

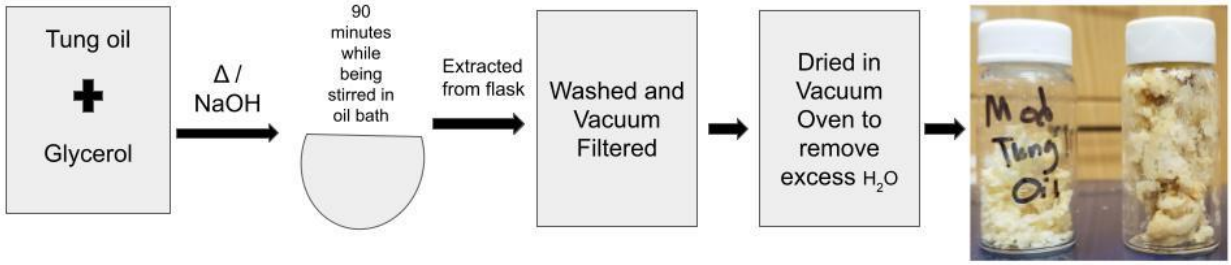

Figure 16: Pictorial diagram of the modification of tung oil with glycerol into Tung Oil Diglyceride (TDG).

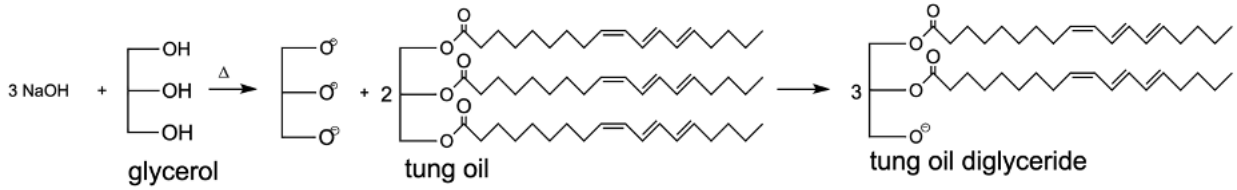

Scheme 2: Schematic diagram of transesterification of tung oil with glycerol and NaOH to form tung oil diglyceride. The H_2O by-product has been washed and vacuumed dried to rid the compound of excess. Stoichiometric calculated to be 3:2:1; NaOH:tungoil:glycerol.

The transesterification of tung oil had specific stoichiometric measurements. **Scheme 2** is the overview of the molar ratio of 3:2:1 (NaOH:tungoil:glycerol) that was derived by calculating the mols of tung oil and measurements were carried out from that for NaOH and glycerol. **Figure 16** is a pictorial diagram of the reaction process for tung oil diglyceride. The methodology for the reaction is adapted from Vetkansan et al. using transesterification to modify the tung oil triglyceride into a diglyceride. There are two steps to this reaction. First, the glycerol and NaOH are added to the round bottom flask and stirred for five minutes to initiate the reaction on an unheated stir-hot plate. Once the tung oil was added to the flask the solution was stirred while heating at 65 ℃ in a mineral oil bath for ninety minutes. After the reaction, the tung oil diglyceride (TDG) was vacuum filtered and washed with acetone and water to remove excess unnecessary acid chains and salts. After analyzing the TDG with FTIR, there was a huge peak indicating water still present within the molecule. Subsequently, the product was further dried in the vacuum oven at 70 ℃ for twenty-four hours to remove excess water. The compound came out to be a pale white to off-white thick paste (**Figure 16**). There are two vials present in **figure 16**. Both are labeled, but one has been turned around for better visibility of tung oil diglyceride compound.

2.3.1 Fourier Transmission Infrared and Raman Spectroscopy

Figure 17 has two FTIR spectrums of tung oil diglyceride that were stacked for comparison. The excess water in TDG is expressed in the top graph. The peak in question is not the 3500 cm^{-1} to 3000 cm^{-1} peak. This was expected due to modification of the triglyceride to a diglyceride. However, the unexpected peak actually occurred at 1559 cm^{-1}. This peak is drastically reduced after a drying cycle in the vacuum oven. The representational peaks for TDG follow the same spectrum details seen in tung oil which are 1734 cm^{-1} (carbonyl) and 2929 cm^{-1} (Csp^3-H). The comparison from tung oil to tung oil diglyceride can be seen in **figure 26**.

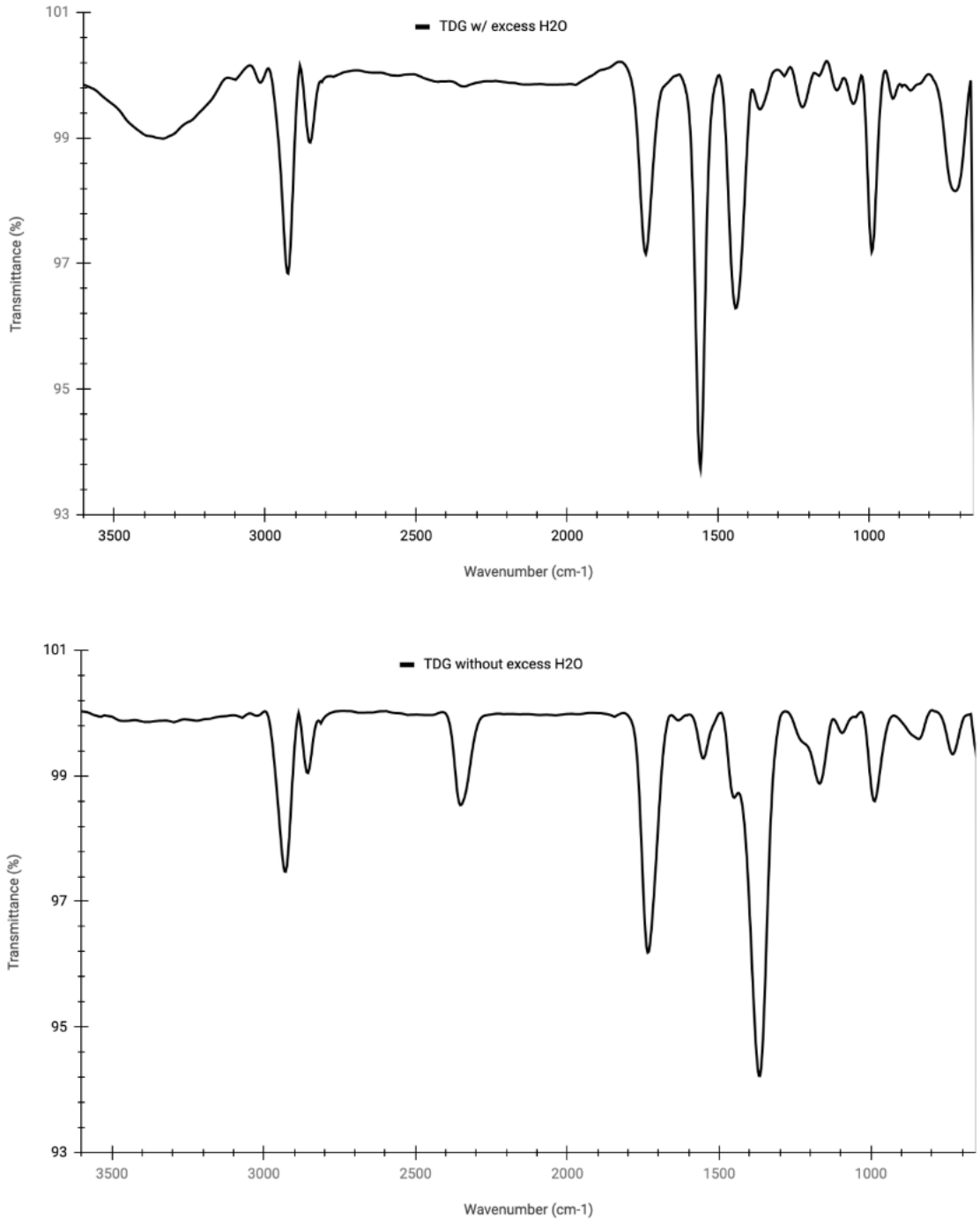

Figure 17: Fourier Transmission Infrared spectrum of tung oil diglyceride comparing the compound's peaks with and without excess H_2O.

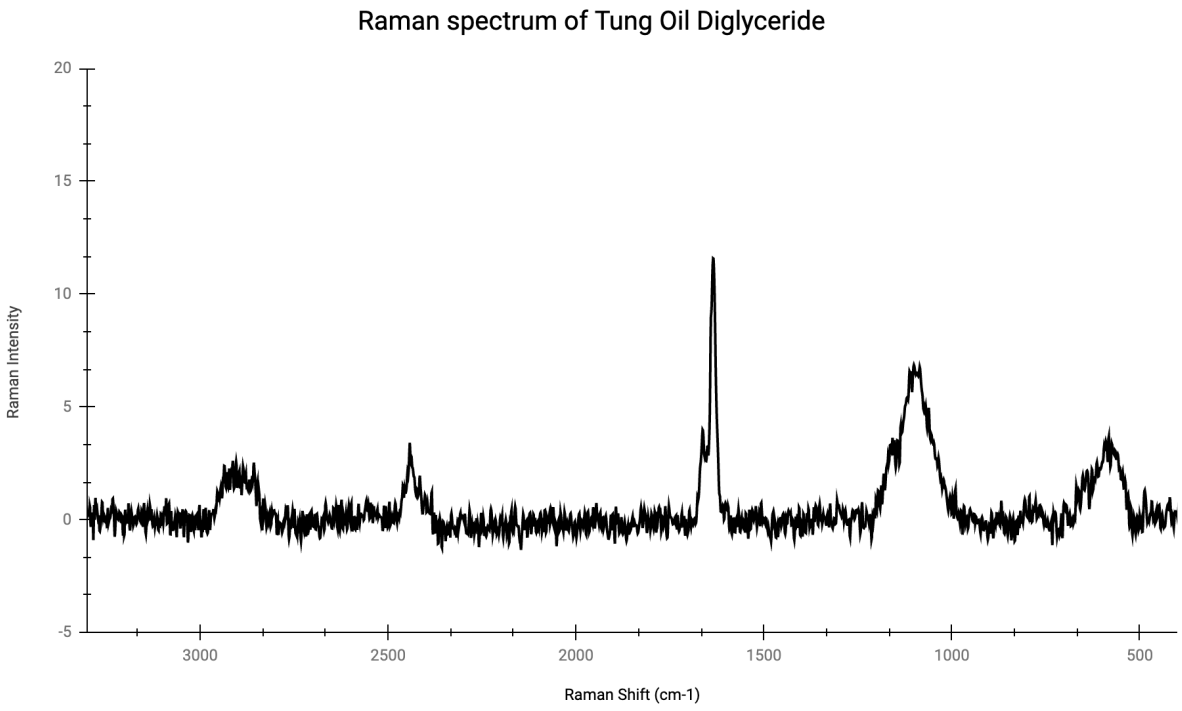

Figure 18: Raman Spectra of the formed tung oil diglyceride.

Raman spectroscopy was also performed on TDG for supporting characterization. The peak at 1640 cm^{-1} continues to be produced in the spectrum which reinforces the modification of the triglyceride to a diglyceride did not affect the conjugation in this step of the monomer formation. This conjugation is necessary for the free radical reaction to propagate the monomer into a polymer once initiated.

2.3.2 Nuclear Magnetic Resonance

The ^{1}H proton spectrum in **figure 21** for TDG was enhanced to showcase the peaks 4.2 ppm, 4.35 ppm, 5.25 ppm and collection of multiplets from ~5.40 to 6.45 ppm reinforcing there is no major change in functionality or formation to the diglyceride. The peaks mentioned above are the same peaks that are found in the original tung oil that represent the esters, hydrocarbon backbone and conjugation.

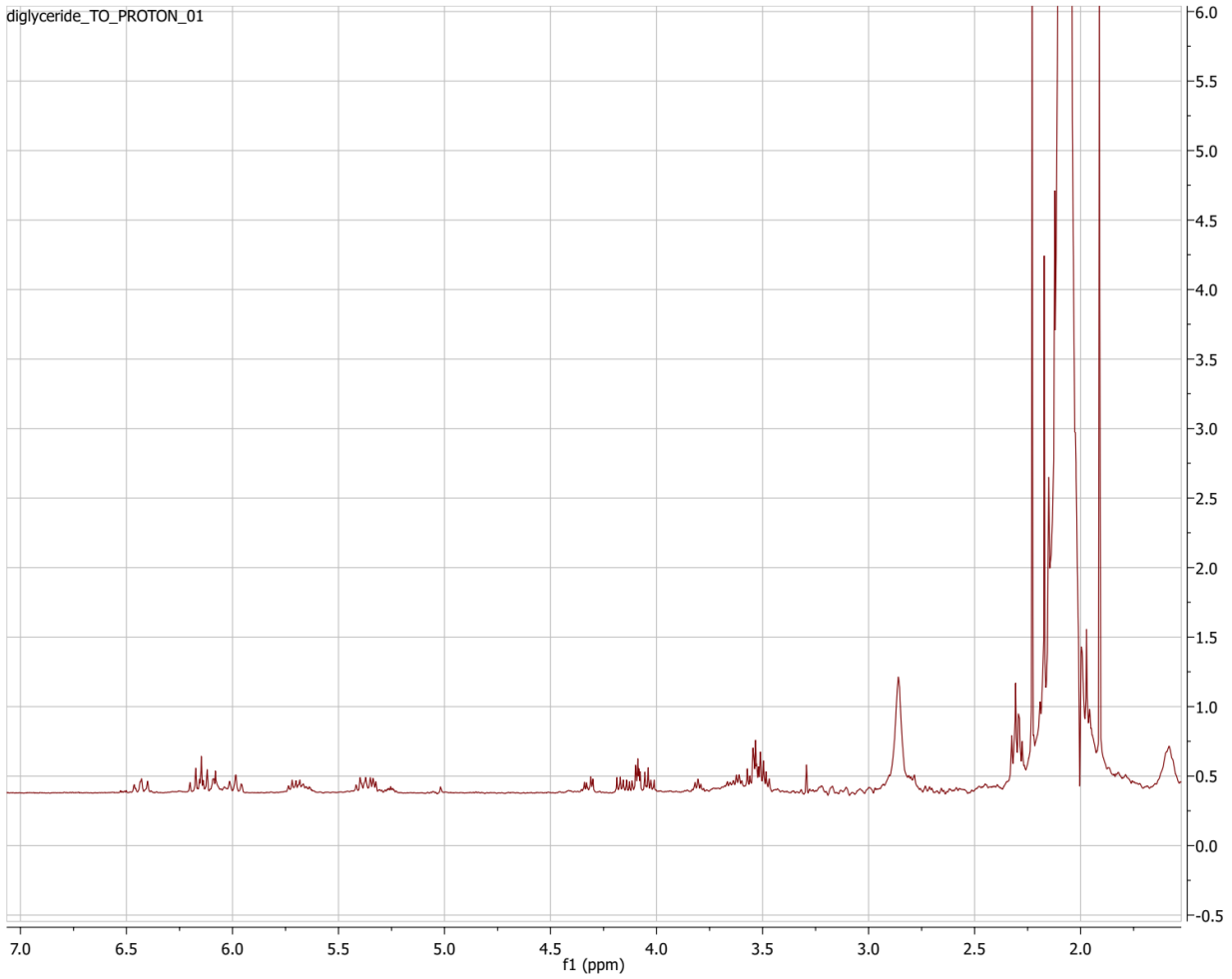

Figure 19: Nuclear Magnetic Resonance spectrums of ^{1}H of tung oil diglyceride.

2.3.3 Gas Chromatography and Mass Spectroscopy Analysis

Regrettably, this is a clean spectrum that came from running a sample of TDG with the same parameters used to run pine rosin and tung oil. However, the data is inconclusive as a consequence of the starting materials not able to produce clean GCFID-MS data to be able to compare the differences.

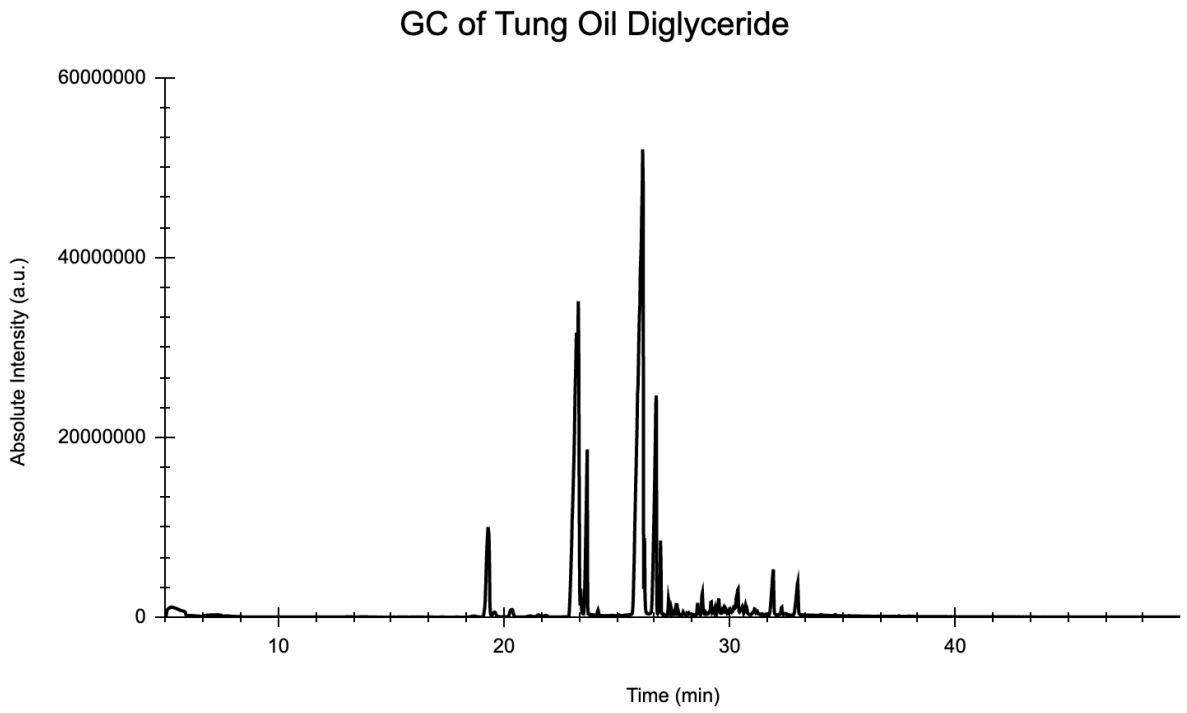

Figure 20: Gas Chromatography spectrum of tung oil diglyceride using absolute intensity over time.

2.3.4 Thermal Gravimetric Analysis

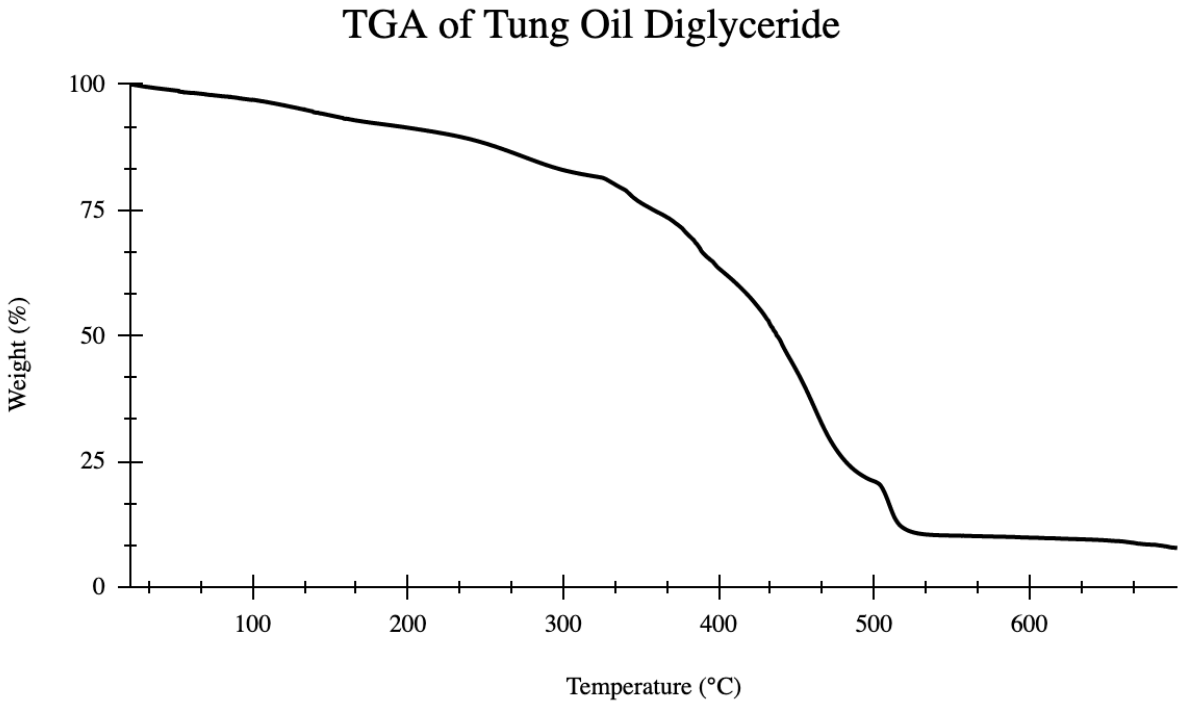

Figure 21: Thermal Gravimetric Analysis of the first step of the monomer – tung oil diglyceride.

Tung oil diglyceride's thermal gravimetric analysis graph is not as smooth in appearance as its predecessor, tung oil. This could be due to minimal amounts of water byproduct still being present in TDG. However, it is not a cause for concern. In **figure 21** the thermal degradation point for TDG met expectations being above 300 ℃.

2.3.5 Differential Scanning Calorimetry

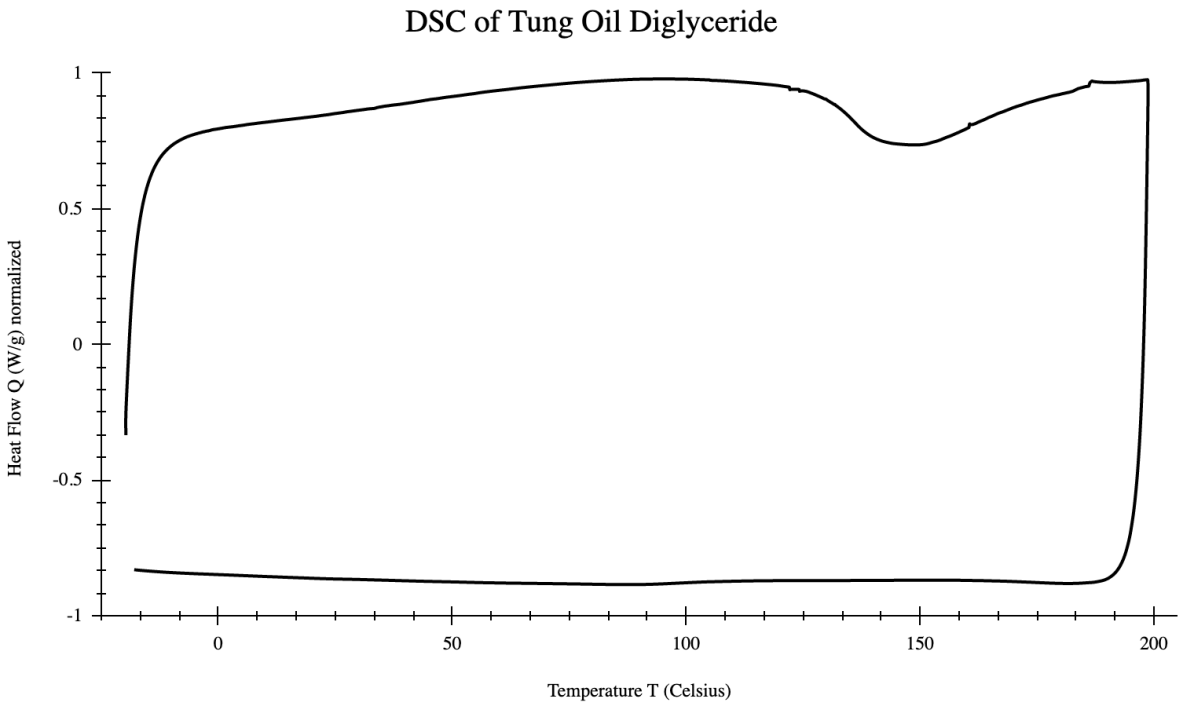

Figure 22: Differential Scanning Calorimetry analysis of tung oil diglyceride.

The DSC run of the TDG seems to run concurrently with the prior runs with the starting materials. There was a heating curve downward depicted in **figure 22** that occurs ~145 ℃. Even though this happened, looking back at the differential scan for tung oil there was a similar dip at ~110 ℃ to ~145 ℃. The sample was heated to 200 ℃ for consistency throughout prior measurements.

2.4 Reaction of Pine Rosin with Acid Esterification

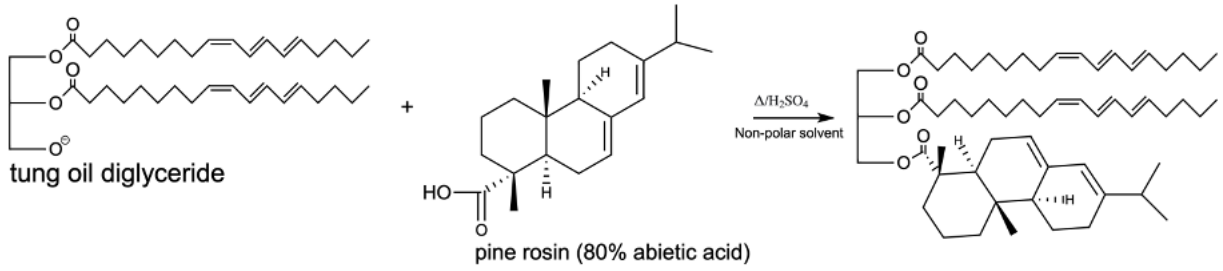

Scheme 3: Schematic of acid esterification of pine rosin (>80% abietic acid) being attached to the tung oil diglyceride.

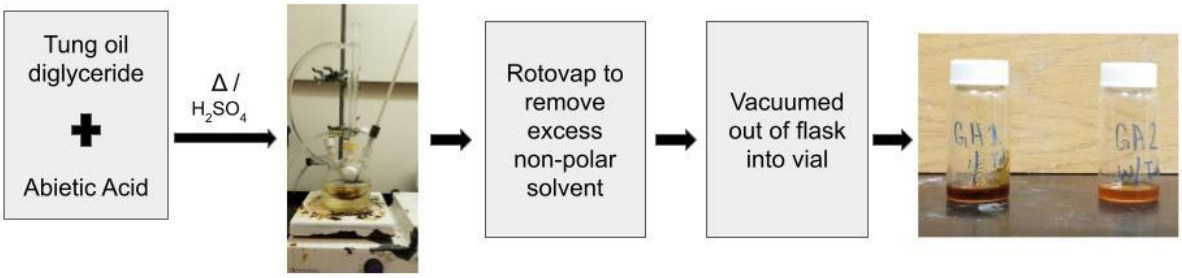

Figure 23: Diagram of the process for the second step of Tung Oil Abietate monomer formation.

The methodology follows the study by Venkatesan et al. using an acid catalyst to attach the pine rosin to the TDG through esterification. The stoichiometry changes for this step to a 1:1 ratio of tung oil diglyceride to pine rosin due the molar mass weight change in tung oil once it was modified into a diglyceride. Tung oil diglyceride's molar mass was calculated to be 612 g/mol. Sulfuric acid was used as a catalyst and added as a 1:1 ratio with pine rosin through the molar mass of tung oil diglyceride. The pine rosin was first added to toluene, a non-polar solvent to make a solution, secondly adding concentrated sulfuric acid (H_2SO_4) (**Scheme 3**). Prior to adding H_2SO_4, the pine rosin and toluene solution were stirred in the round bottom flask for five minutes. Once the H_2SO_4 was added and stirred for another five minutes, the TDG was added to the round bottom flask to complete the reaction through a stirred heating process at 55 °C for 150 minutes. To ensure that the toluene had been depleted from the reaction,

the tung oil abietate (TOA) went through rotary vaporization to remove excess. Whereas the TDG was a pale, off-white paste-like sticky compound, after completing the reaction the TOA was a deep dark viscous compound (**Figure 23**).

2.4.1 Fourier Transmission Infrared and Raman Spectroscopy

Figures 24 and **25** are the original FTIR and Raman spectrums of tung oil abietate. These two spectrums have been incorporated into **figures 26** and **27** to compare the transition of the starting materials into the formation of tung oil abietate and its polymerization. There are two distinct FTIR peaks, ~2900 cm^{-1} and ~1750 cm^{-1}, in **figure 26** that are consistent in every IR spectrum except glycerol. These peaks reinforced structural consistency in the formation of tung oil abietate. Mentioning glycerol, the hydroxyl peak that is well known to be located from 3500 cm^{-1} to 3000 cm^{-1} has a huge broad peak in spectrum 2. This peak was not in any other spectrum except tung oil diglyceride seen in spectrum 3 of **figure 26** which is to be expected after the first step of the transesterification with tung oil and glycerol.

Figure 27 has five different Raman spectrums that compare the transition of pine rosin and tung oil into tung oil abietate as well as the polymer formed with TOA. The one distinct peak around 1640 cm^{-1} is displayed throughout the first four peaks. Unfortunately, there was an issue with the x-axis when formatting the stacked spectra figure. The peak at 1640 cm^{-1} located in spectra 1, 2 and 4 looks shifted to ~1800 cm^{-1}. In the original spectrums of each material the peak is located around ~1640 cm^{-1}.

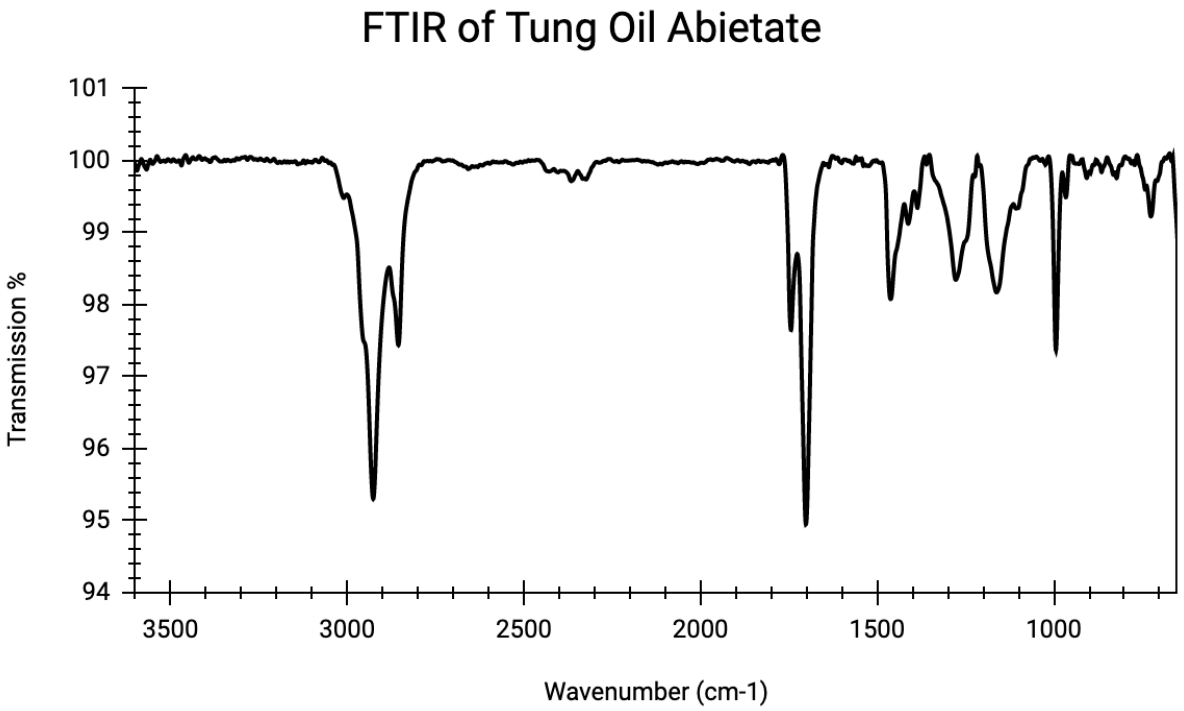

Figure 24: IR spectrum of Tung oil abietate.

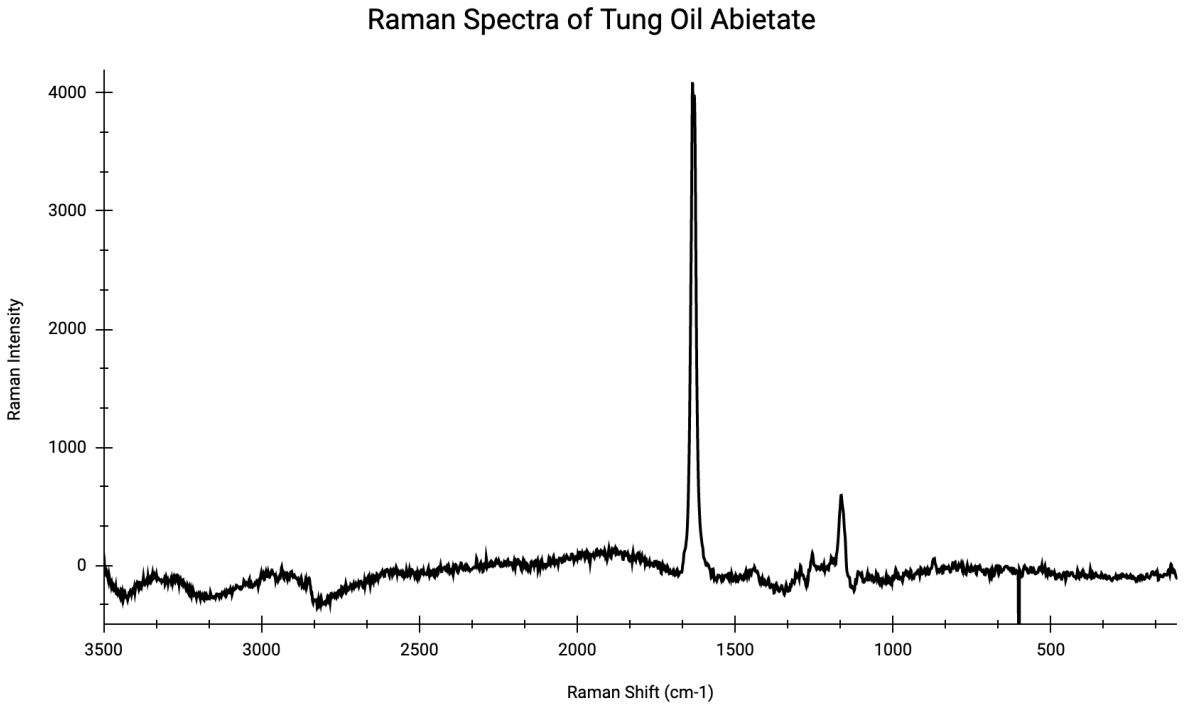

Figure 25: Raman spectrum of the entire monomer, tung oil abietate.

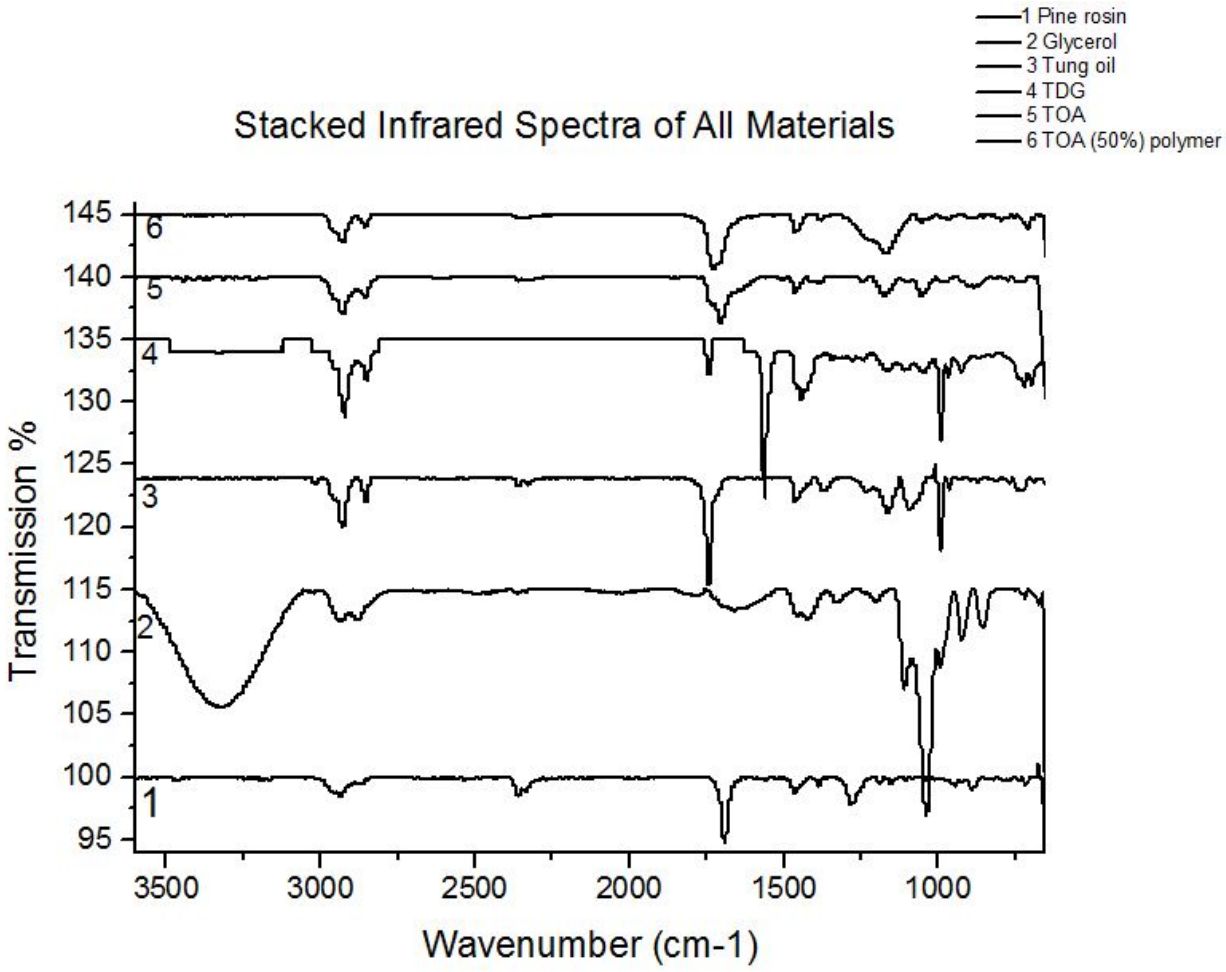

Figure 26: Stacked spectra Fourier Transmission Infrared analysis of the starting materials transition into the Tung Oil Abietate.

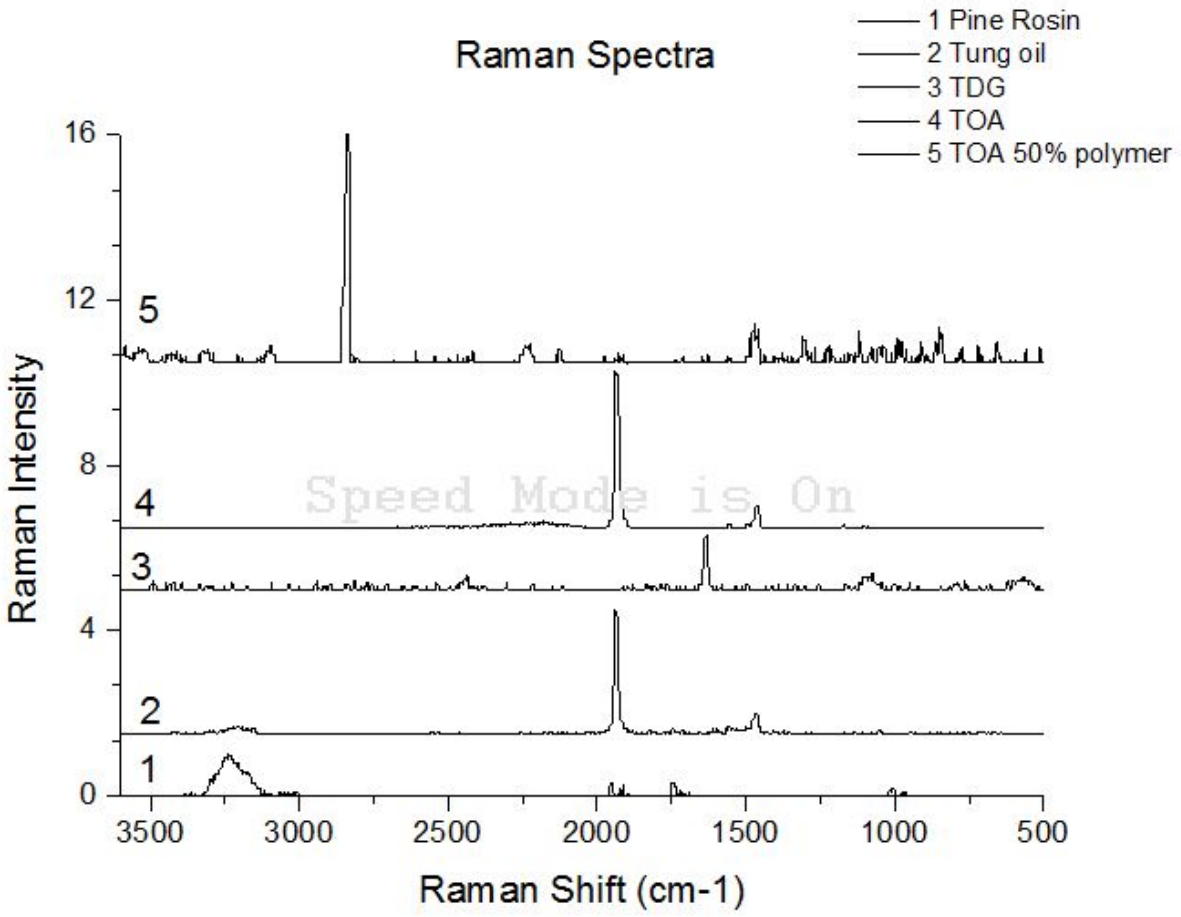

Figure 27: Raman Spectra of all the materials used and constructed to synthesize tung oil abietate (TOA).

2.4.2 Nuclear Magnetic Resonance

The ^{1}H NMR spectrum in **figure 28** has two expanded graphs, A and B, that point out consistency of the glycerol backbone and conjugation with the formation of the novel monomer. The peaks at 4.2 ppm, 5.25 ppm and collection of multiplets from 5.35 ppm to 6.45 ppm are the same peaks that have transitioned from tung oil and tung oil diglyceride to formation of the tung oil abietate. Depicted in **figure 28** the absence of the peak in the circled up field area of 10 ppm to 11 ppm provided confirmation that the carboxylic acid is no longer in the molecule.

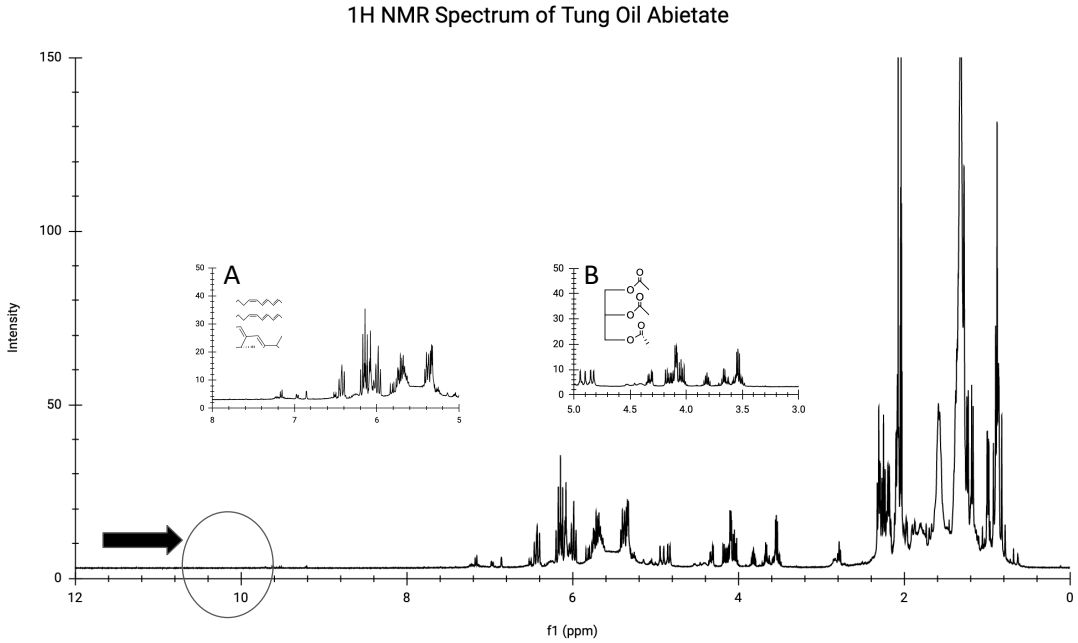

Figure 28: Nuclear Magnetic Resonance spectrums of ^{1}H proton spectra of tung oil abietate.

2.4.3 Thermogravimetric Analysis of Tung Oil Abietate

Continuing suit with thermal gravimetric analysis, **figure 29** illustrated TOA having a high degradability rate. The novel monomer does not begin to degrade heavily till about 350 ℃ which was higher than pine rosin alone that degraded between 220 ℃ and 240 ℃. It appears the thermal stability steadily increased during the formation of TOA.

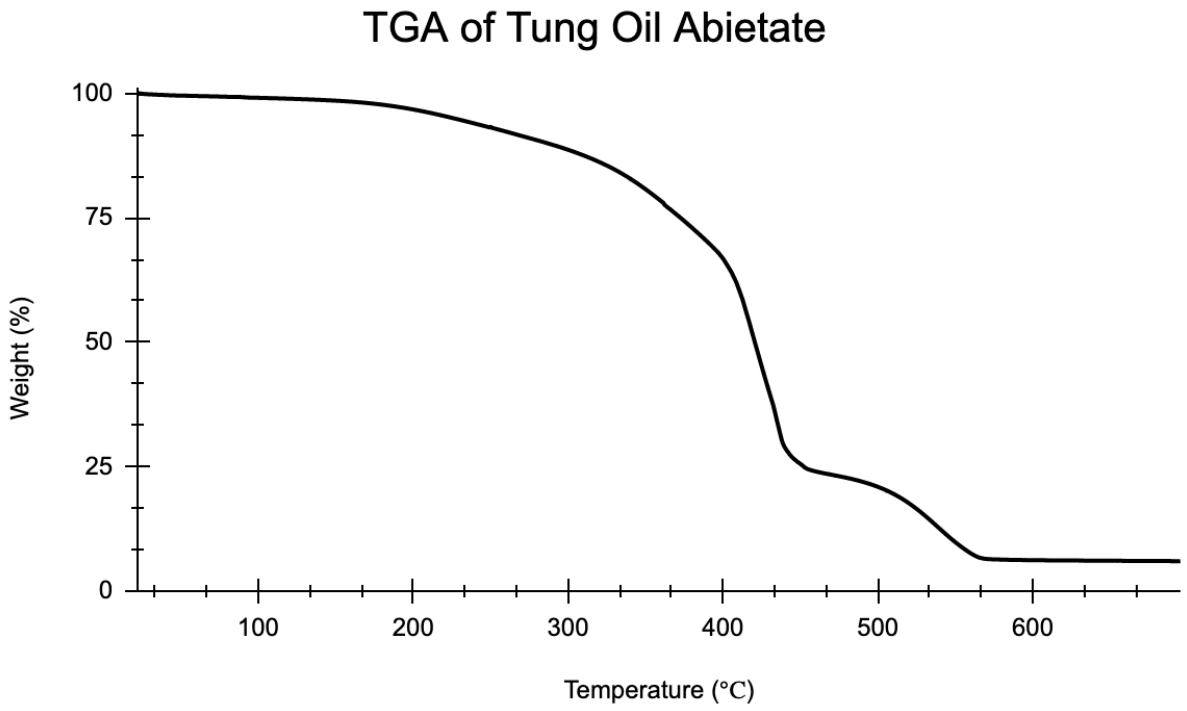

Figure 29: Thermal Gravimetric Analysis of the tung oil abietate (TOA) finished monomer.

2.4.4 Differential Scanning Calorimetry

In **figure 30** below, the tung oil abietate did not have any major exothermic or endothermic spikes. There does not appear to be any phase changes either. Looking back at all the DSC graphs there was consistency overall. Pine rosin DSC graph did show some phase changes. Tung oil did not appear to have any phase changes or exothermic/endothermic spikes. After formation of TDG, the DSC graph did have a slight phase change, but it was not overly significant. All prior runs were done till 200 ℃, but TOA was heated till 400 ℃ which runs concurrent with the thermal gravimetric analysis temperature profile. The chosen temperature point helped support the high degradability point from the TGA measurement.

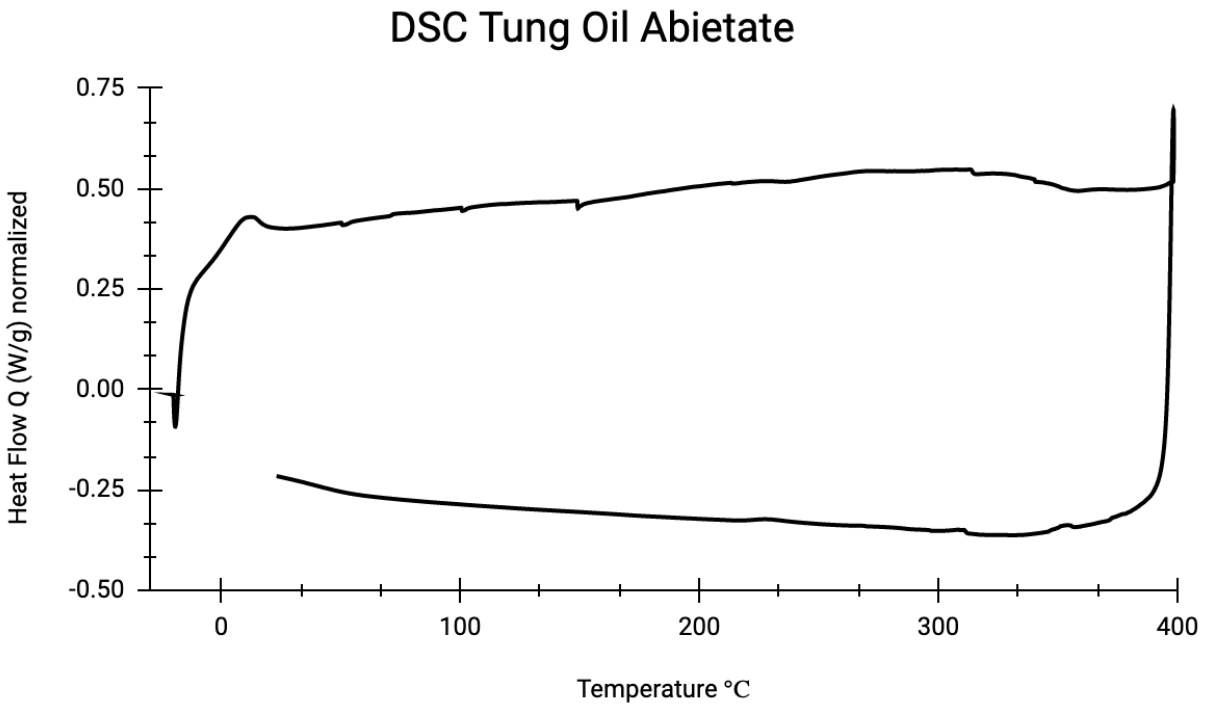

Figure 30: Differential Scanning Calorimetry spectrum of tung oil abietate.

2.5 Discussion

During the monomer preparation, two types of non-polar solvents were chosen at first to see which would be best to dissolve the pine rosin. These were hexane and toluene. Toluene was the first choice due to its high boiling point at 110 ℃ which would allow the monomer formation to occur during the heating process. Pine rosin is also known to dissolve in toluene. After preparing the monomer for the first time, it had a heavy smell that lingered from the toluene. To alleviate the odor from toluene, the monomer sample was place in the rotary vaporization instrument at 110 ℃. This had to be watched carefully as to not burn the sample. The other solvent chosen was hexane after toluene in hopes to alleviate the need to go through a rotary vaporization step. The hexane proved to be more problematic with a boiling point at 69 ℃. The hexane did not produce a good monomer sample. It is not entirely clear why the lower boiling point or the solvent did not do well with the TOA monomer formation since the heating temperature for the

reaction was at 55 ℃. Therefore, toluene was kept as the non-polar solvent and rotary vaporization helped alleviate any leftover toluene solvent and odor.

CHAPTER 3

POLYMERIZATION OF TUNG OIL ABIETATE

To polymerize the novel monomer Tung Oil Abietate (TOA), the following materials were used to do so. The TOA was synthesized in the lab of the Chemistry and Biochemistry Department of Georgia Southern. The additional materials n-butyl methacrylate (BMA) and Luperox (di-tert-butyl peroxide DTBP) were purchased from Sigma-Aldrich (St. Louis, MO) and the divinylbenzene (DVB) was purchased from TCI America (Portland, OR). The Yamato DKN 600 convection oven was used to cure polymer samples. Fourier Transmission Infrared Spectroscopy (FTIR) was performed on the Thermo iS10 FTIR with the Smart Stage attachment (Waltham, MA). Thermal properties were measured on the Texas Instruments Q50 TGA and TA Instruments Q100 DSC w/ cooling unit (New Castle, DE).

3.1 Free Radicalization

Literature denotes several polymerization approaches that could be used to polymerize TOA such as polycondensation, ring opening metathesis polymerization (ROMP) and free radical polymerization (FRP).[4,8,10,17] Due to its molecular size, pine rosin would require modification for polycondensation.[4] ROMP has polymerized rosin acids, but once again the monomer was first isolated then modified with other functional monomers.[2,4,17] FRP was chosen for TOA which allowed the ability to take full advantage of the novel monomer's functionality as well as the least amount of modification. Unlike ROMP, the free radical approach is overall greener with lower temperatures, less reaction time and little to zero solvent usage, thus reducing time and waste.[10,18]

Tung oil was modified into a diglyceride, but only to form a novel monomer with pine rosin (>80% abietic acid). There were no prior modifications to pine rosin before esterification with tung oil diglyceride. With the addition of the pine rosin to the tung oil diglyceride, the rosin acid adds functionality to the novel monomer with the carboxylic acid and conjugation in the second and third rings in the molecule that have reactive sites that aid in the free radical approach.[4,10] Yanju et al. uses FRP to

polymerize a rosin derivative stating that conjugated C=C bonds are easier to polymerize unlike unconjugated C=C and derive higher molecular weight polymers.[10]

Depicted below in **scheme 4** is the overall reaction on how radicalization would occur to form a linear polymer. In general, there are three steps in FRP, initiation, propagation and termination.

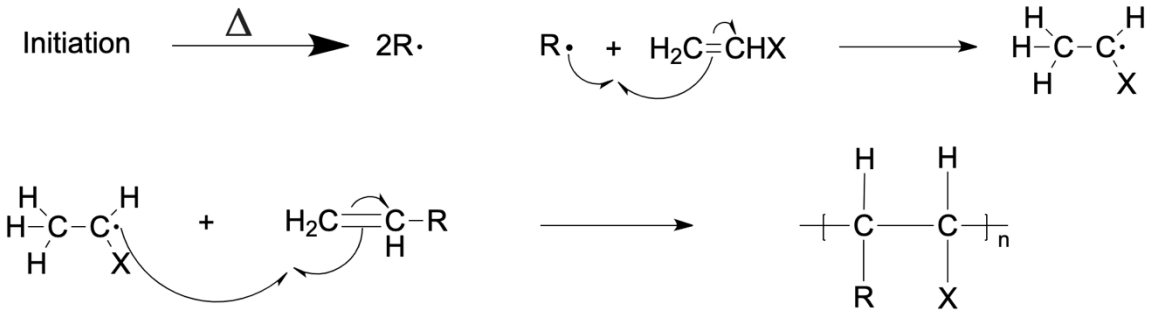

Scheme 4: Generalized schematic of Free Radical Polymerization.

From prior literature tung oil can be polymerized due to the triple conjugation of the **α**-eleostearic fatty acid chains and can be polymerized by itself.[8] However, due to surrounding fatty acids within the triglyceride causes lower reactivity time.[8] To aid in reaction capabilities, BMA and DVB are used as co-monomers in the overall polymerization of tung oil abietate (**Figure 31**). BMA structurally has heightened vinyl reactivity due to the attached ester group and DVB compliments and balances with the aromatic resonance that helps push the radicalization reaction (**Scheme 6**).[8]

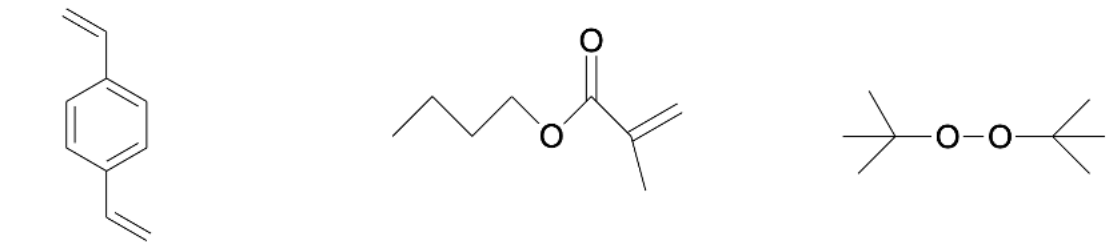

Figure 31: Chemical Structure of divinylbenzene (DVB), n-butyl methacrylate (BMA) and di-tert butyl peroxide (DTBP). The first two are the co-monomer additions and the last is the free radical initiator.

3.2 Methodology

TOA polymer was prepared using 5.0 mg of TOA, 3.0 mg of BMA and 2.0 mg of DVB placed into a new 20 mL vial (**Figure 31**). Adapted from prior literature that used a 3:2 ratio of BMA:DVB allowed samples to be made with different percentages to find the optimal recipe.[8] The 0.5 g of DTBP initiator was added last. All materials were gravimetrically weighed on an analytical balance for accurate measurement. The prepared sample was vortexed for thirty seconds to achieve a homogenous mixture. Next the sample was placed into the convection oven for 18 hours at 140 ℃. This was done under a two-step program that allowed time for the oven to ramp up to 140 ℃ for 15 minutes. All other samples were prepared in the same manner.

3.2.1 Results and Discussion

Table 1 outlines the nine samples prepared. The first sample in **table 1** was made from the adapted recipe that included the 3:2, BMA:DVB ratio. After this sample appeared to have success in polymerizing, the next step was to make samples in percentage intervals and test them for their thermal properties. The second and third samples were made in a five percent increase in the amount of TOA following the first sample. This was done to test for any characteristic influx in between a five percent increase of the samples prepared. The fourth and fifth samples were made in ten percent incremental measurements after the first three appeared to have no issues with an increase in TOA monomer percentage. All five samples came out completely hardened and in a darker color than any of the prior materials. The last four samples were made in five percent increases to know what the limitations were of the sample's recipe. All samples came out similar in color, but not hardness. The first six samples were overall quite hard and tough. Sample seven (90:6:4) and eight (95:3:2) were more flexible due to the lessened BMA:DVB ratio that would cause less cross linkage to occur, but they were fully polymerized from appearance and

touch. Sample nine at 100 percent TOA with only DTBP did harden and was solid to the touch, but it was far more flexible. Further characterization will need to be done on the last three samples to analyze for quality and property to see if they are viable for future investigation. The first six samples appear to be ready for future work with dielectric analysis and dynamic mechanical analyzation.

Table 1: Polymerized tung oil abietate ratio recipes with BMA and DVB for nine samples.

50:30:20	70:16:12	90:6:4
55:27:18	80:12:8	95:3:2
60:24:16	85:9:6	100:0:0

Scheme 5 is a diagram of the generalized free radical approach with initiation and propagation of TOA with the initiator DTBP. This diagram does not include BMA and DVB for clarity. In **scheme 6**, the fully polymerized TOA does have BMA and DVB incorporated into this diagram to see that all conjugated double bonds have been replaced. The double bonds break due to the radical causing the electron to be shared with the radical thus forming a new covalent bond. Subsequently, this step repeats itself until all electrons have been used from the available pie system in the conjugated C=C bonds. Termination occurs once that has happened.

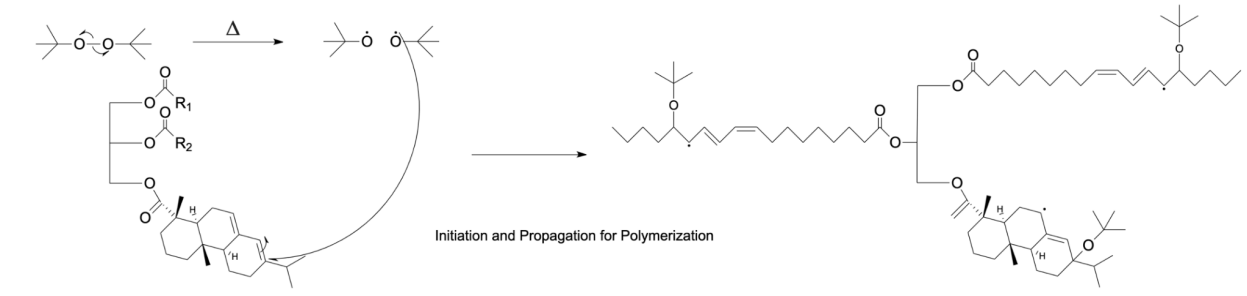

Scheme 5: General schematic of the free radical polymerization of tung oil abietate. This diagram does not include BMA and DVB.

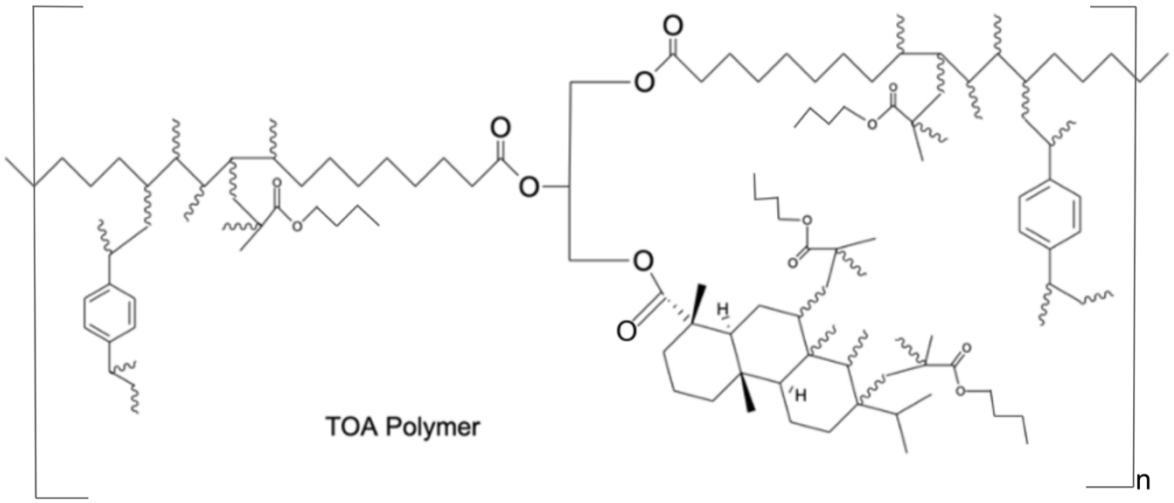

Scheme 6: Diagram of the polymerized Tung Oil Abietate with BMA and DVB crosslinking co-monomers located at the original site of conjugation.

3.3 Characterization Analysis

3.3.1 Fourier Transmission Infrared and Raman Spectroscopy

To identify polymerization efficiently and quickly, the FTIR and Raman instruments were used to analyze the TOA polymer samples. **Figure 32** is a collection of IR spectrums, and it displays the absence of conjugation peak ~1625 cm^{-1}. This is reinforced with the Raman spectrum of the TOA polymer in **figure 33** that is void of that conjugation peak at 1650 cm^{-1} to 1640 cm^{-1}. The absence of these peaks in FTIR and Raman support that conjugation has been fully propagated and polymerized when cured during the reaction. In the spectrum of the polymer there is a new peak ~1450 cm^{-1} that represents the aromatic ring found in DVB. The largest peak between 1750 cm^{-1} and 1700 cm^{-1} runs congruent with the starting materials, tung oil diglyceride, tung oil abietate and BMA. This peak represents the C-O stretch found in the esters that are throughout this polymer chain. Following the spectrum of **figure 32**, it supports the structural peaks that were in both pine rosin and tung oil such as the Csp^3-H peak at 2900 cm^{-1} 2800 cm^{-1}.

This spectrum reinforces that all compounds used were not modified prior to use in any of the reactions that have been performed during this research.

The peak that is in **figure 33** is ~2550 cm^{-1} which is likely due to the S-H stretch caused from the sulfuric acid used to esterify the pine rosin's carboxylic acid. There were no other significant peaks in the Raman data.

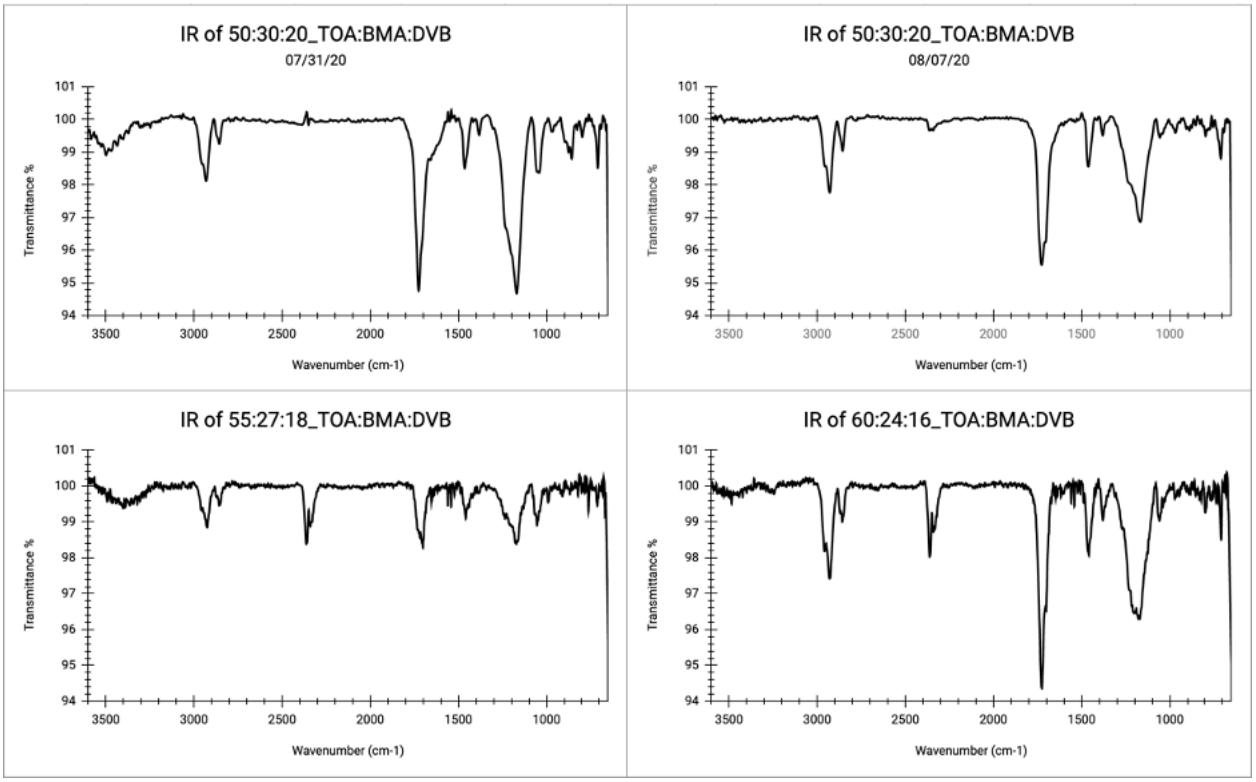

Figure 32: IR spectrums of polymerized Tung Oil Abietate monomer.

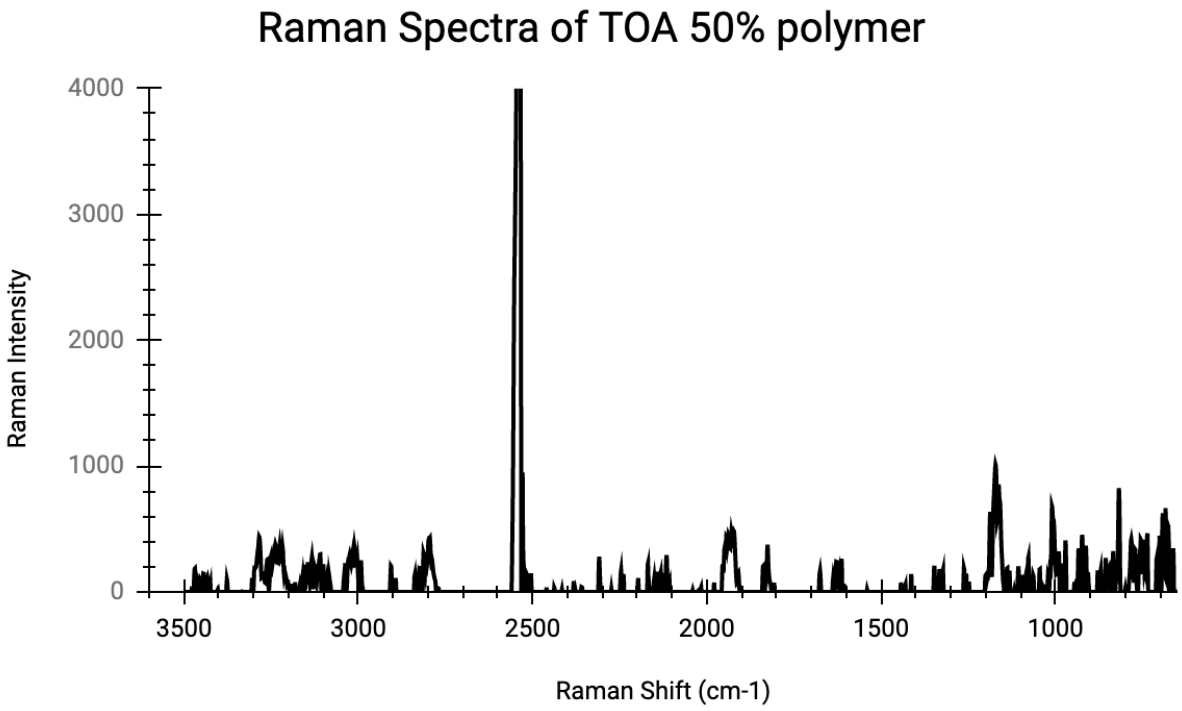

Figure 33: Raman Spectrum of tung oil abietate polymer that consists of 50% TOA monomer in the polymer matrix.

3.3.2 Thermal Gravimetric Analysis

Figure 34 depicts a collection of TGA measurements of three polymer samples at three different percentage additions of the TOA monomer within the prepared polymer samples. There are four graphs but two are repeats for consistency in measurement. All four graphs show the three percentages hold a high degradability at >350 ℃ that strengthen the stability of the TOA polymer. These thermal measurements aid in the continuation of future work with the TOA polymer as well as pine rosin in other areas of material and organic research.

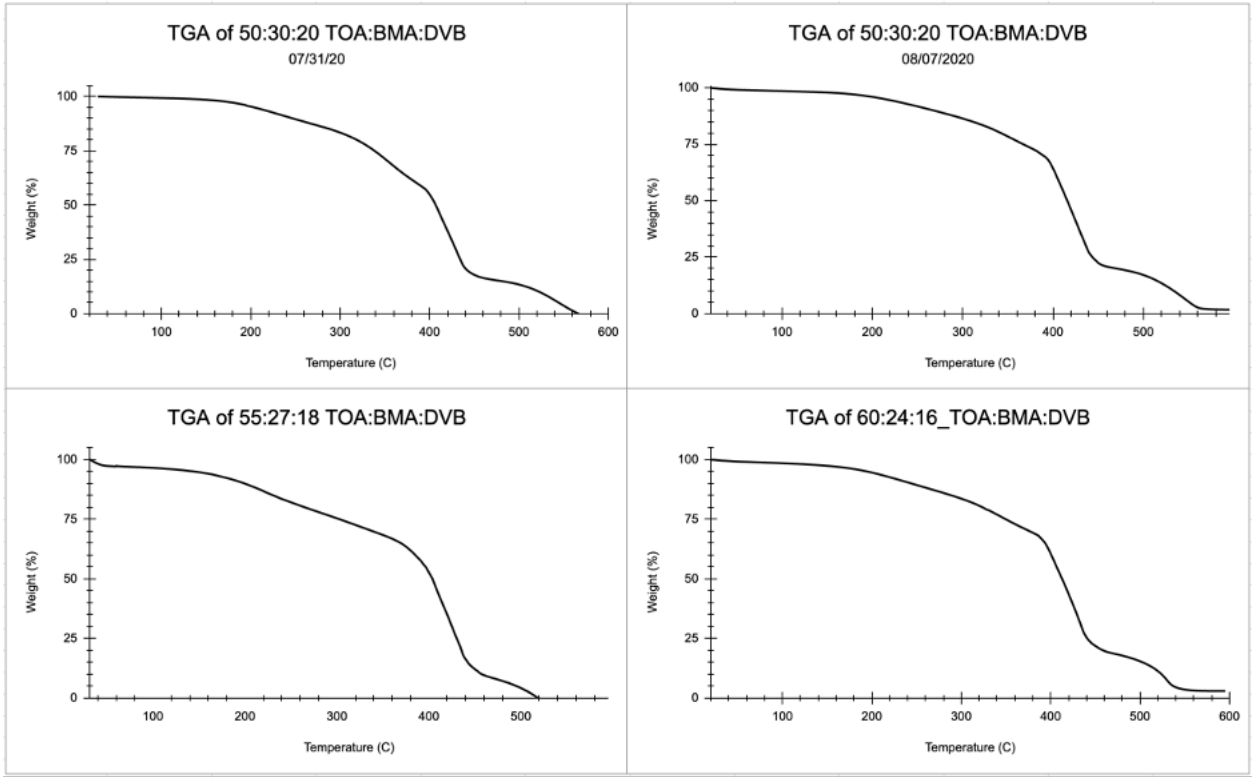

Figure 34: Thermal Gravimetric Analysis of the polymerization of Tung Oil Abietate.

3.3.3 Differential Scanning Calorimetry

During the polymerization of TOA, a few of the early samples appeared to not cure correctly from the first DSC scans. Those measurements were made with a heating-cooling cycle of 20 ℃/min to 200 ℃ and back down to 20 ℃. To see if there were issues with the curing reaction, DSC was running again on polymer samples that were measured to 160 ℃ with a heating-cooling-heating cycle to quickly identify any abnormalities (**Figure 35**). The chosen temperature is twenty degrees higher than the curing time for the samples for that reason.

To better understand the graphs in **figure 35**, the four samples went through a heating-cooling-heating cycle with a constant 20 ℃/min ramp to 160 ℃. The cycle started with a -20 ℃ equilibrium and heated from there. After that the cooling went back down to 20 ℃ and the last heating cycle went from 20

℃ to 160 ℃. All samples were relatively the same in weight averaging 8 mg and placed in the same type of standard measuring pan. When the pans were retrieved from the crucible area, they were all intact and not compromised. Unlike prior scans, these samples do not appear to have any cause for concern with curing temperatures. In the first graph there is a small peak during the cooling cycle ~75 ℃. However, in the identically prepared sample in the second graph there are no thermal physical changes. In the bottom two graphs there are two peaks that occur ~60 ℃ to 70 ℃ with no other reoccurring peak in the next two temperature cycles indicating what could be a release of energy to allow balance of heat flow with the reference pan.

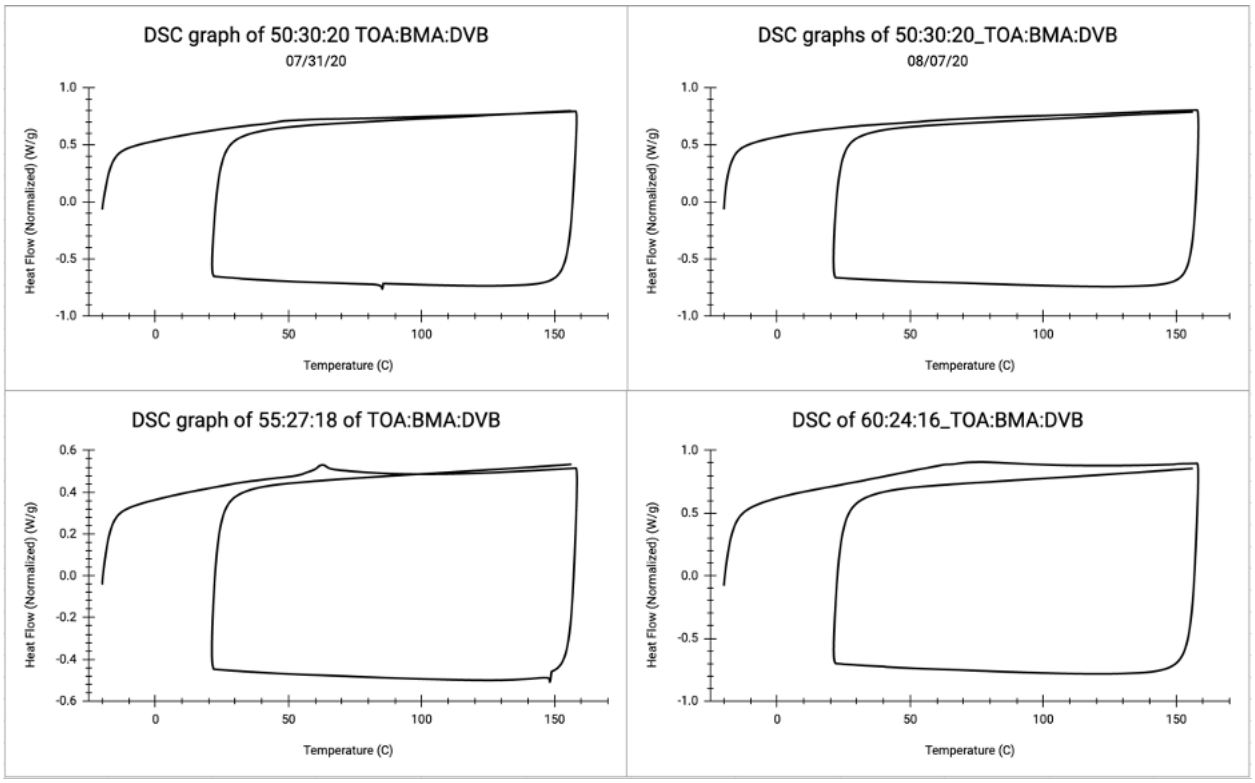

Figure 35: Differential Scanning Calorimetry for TOA polymer with BMA and DVB incorporated.

CHAPTER 4
CONCLUSION

Originally, pine resin (aka pine sap) was explored for a polymeric possibility. The aim was to use a regionally and locally sourced non-edible plant for a polymer that could facilitate the reduction of petrochemical usage and support the agricultural industry. The initial studies were performed on pine resin and its two fractions; turpentine and pine rosin, in which the data yielded support for the importance of further studies with pine rosin.

Conclusively, from FTIR, Raman, ^{1}H and ^{13}C NMR identification, pine rosin contains the monomer abietic acid which became the focus of the research and how it should be polymerized. From prior literature, the abietic acid had been studied by isolating it from pine rosin and altering the monomer for epoxies, adhesive and ink polymers.[4,10] Natural abietic acid that had been isolated from pine rosin had been used to form a fully bio-based epoxy.[11] No literature was found that fully polymerized pine rosin without first isolating a desired molecule within pine rosin for thermoplastics or thermosets. However, material property tests were executed on the TGA and DSC that reinforced pine rosin had sound thermal and physical properties that can be useful for polymer formation. This thesis provides conclusive data that it is possible to polymerize pine rosin. The research path grew over time to develop a novel monomer with tung oil and abietic acid together. Tung oil is a renewable non-edible plant which further enhanced the green approach as well as enhancing the novel monomers thermal properties.

The formation of Tung oil abietate comes from two mechanistic steps. Tung oil was modified into a diglyceride by transesterification. Subsequently, the successful modification of tung oil was identified through FTIR, Raman, ^{1}H and ^{13}C NMR and GC. The second step involved attaching the pine rosin through esterification by using the carboxylic acid. TOA went through characterization as well with FTIR, Raman, ^{1}H and ^{13}C NMR and GC to ensure the formation of the novel monomer. Tung oil diglyceride and tung oil abietate were tested for their thermal and physical properties on the TGA and DSC during production.

Transesterification and esterification were the mechanisms employed to synthesize the novel monomer, and they did not generate a harmful by-product doing so. Subsequently, using those specific mechanisms it was possible to provide an environmentally friendly and renewable monomer from tung oil and pine rosin.

Scheme 2 is the overall idea to construct the novel tung oil abietate that originated through a stoichiometric ratio deriving from the molecular weight of tung oil. The first step to modify tung oil involved a 3:2:1 ratio of NaOH:tung oil:glycerol (**Scheme 1**). For the second step to occur, the ratio changed to a 1:1, but this is 1 mol of tung oil diglyceride to 1 mol of pine rosin (**Scheme 2**). The second calculation for the new stoichiometric measurement was based through the molecular mass of tung oil diglyceride.

Divinylbenzene (DVB) and n-butyl methacrylate (BMA) were used for thermomechanical enhancement as co-monomers in the polymerization of TOA (**Figure 31**). Due to time constraints as well as global situations that were out of any person's control, it was not possible to find an optimal curing time for the polymer by dielectric analysis (DEA). Two other limiting factors occurred as well during optimization. The first being the scanning electron microscope (SEM) is currently not working. The second is the GPC/SEC (gel permeation chromatography) instrument utilized to identify molecular weight as well as polymer formation has been down for quite some time. There were attempts to fix the instrument during the beginning of Spring 2020 without success. Though the TOA polymer was limited to identification and characterization with FTIR, TGA and DSC, the duplicated data on the FTIR shows the stretch and vibration peak that represents conjugation in the fingerprint region is no longer in the spectrums. The thermal and physical measurements made with TGA and DSC not only provide sound data that support the use of the TOA polymer, but can be used in the future to help with optimization.

The utilization of pine rosin with tung oil has not been found in any other research as of yet. The novel monomer aims to contribute to the polymer industry and the organic chemistry community. Subsequently, future goals are to enhance the polymers cure schedule with the use of the DEA. The next step will be to find the right ratio by percentage of TOA monomer to added comonomers, BMA and DVB.

Depending on the application, there could be the ability to utilize different percentages of the TOA polymer dependent upon thermomechanical property needs. Considering the research, the data postulates the novel monomer and polymer have promising results for future endeavors toward bio-based polymers that support a reduction in carbon footprint and eco-friendly materials.

REFERENCES

(1) Babu, R. P.; O'Connor, K.; Seeram, R. Current Progress on Bio-Based Polymers and Their Future Trends. Prog Biomater 2013, 2 (1), 8. https://doi.org/10.1186/2194-0517-2-8.

(2) Cardona, F.; Sultan, M. T. bin H. Characterization of Environmentally Sustainable Resole Phenolic Resins Synthesized with Plant-Based Bioresources. BioResources 2016, 11 (1), 965–983.

(3) Choi, G.-G.; Oh, S.-J.; Lee, S.-J.; Kim, J.-S. Production of Bio-Based Phenolic Resin and Activated Carbon from Bio-Oil and Biochar Derived from Fast Pyrolysis of Palm Kernel Shells. Bioresource Technology 2015, 178, 99–107. https://doi.org/10.1016/j.biortech.2014.08.053.

(4) Ganewatta, M. S.; Ding, W.; Rahman, M. A.; Yuan, L.; Wang, Z.; Hamidi, N.; Robertson, M. L.; Tang, C. Biobased Plastics and Elastomers from Renewable Rosin via "Living" Ring-Opening Metathesis Polymerization. Macromolecules 2016, 49 (19), 7155–7164. https://doi.org/10.1021/acs.macromol.6b01496.

(5) Al-Salem, M.; Saha, S.; Sharma, A.; Purkayastha, S.; Pandey, K.; Dhingra, S. In *Plastics to energy: fuel, chemicals, and sustainability implications*; Elsevier, William Andrew: Amsterdam, 2019; pp 365–376.

(6) Venkatesan, H.; Godwin, J. J.; Sivamani, S. Data Set for Extraction and Transesterification of Bio-Oil from Stoechospermum Marginatum, a Brown Marine Algae. Data in Brief 2017, 14, 623–628. https://doi.org/10.1016/j.dib.2017.08.031.

(7) Barde, M.; Celikbag, Y.; Via, B.; Adhikari and Maria L. Auad, S. Semi-Interpenetrating Novolac-Epoxy Thermoset Polymer Networks Derived from Plant Biomass. Journal of Renewable Materials 2018, 6 (7), 724–736. https://doi.org/10.32604/JRM.2018.00116.

(8) Murawski, Amanda, "α-Eleostearic Acid Extraction by Saponification of Tung Oil and Its Subsequent Polymerization" (2017). *Electronic Theses and Dissertations*. 1616.

https://digitalcommons.georgiasouthern.edu/etd/1616

(9) Li, Y.; Xu, X.; Niu, M.; Chen, J.; Wen, J.; Bian, H.; Yu, C.; Liang, M.; Ma, L.; Lai, F.; Liu, X. Thermal Stability of Abietic Acid and Its Oxidation Products. Energy Fuels 2019, 33 (11), 11200–11209. https://doi.org/10.1021/acs.energyfuels.9b02855.

(10) Lu, Y.; Zhao, Z.; Bi, L.; Chen, Y.; Gu, Y.; Wang, J. Preparation and Polymerization of Isopimaric Acid Derivatives. Journal of Applied Polymer Science 2019, 136 (31), 47817. https://doi.org/10.1002/app.47817.

(11) Hasan, A. M. A.; El-Saeed, A. M.; Al-Shafey, H. I.; El-Sockary, M. A.; El-Ghazawy, R. A. I. A Preliminary Study on Liquid Crystalline Epoxy Curatives from Natural Abietic Acid. Egyptian Journal of Petroleum 2019, 28 (1), 127–136. https://doi.org/10.1016/j.ejpe.2018.12.003.

(12) Cuzzucoli Crucitti, V.; Migneco, L. M.; Piozzi, A.; Taresco, V.; Garnett, M.; Argent, R. H.; Francolini, I. Intermolecular Interaction and Solid State Characterization of Abietic Acid/Chitosan Solid Dispersions Possessing Antimicrobial and Antioxidant Properties. European Journal of Pharmaceutics and Biopharmaceutics 2018, 125, 114–123. https://doi.org/10.1016/j.ejpb.2018.01.012.

(13) Beltran, V.; Salvadó, N.; Butí, S.; Cinque, G.; Pradell, T. Markers, Reactions, and Interactions during the Aging of Pinus Resin Assessed by Raman Spectroscopy. J. Nat. Prod. 2017, 80 (4), 854–863. https://doi.org/10.1021/acs.jnatprod.6b00692.

(14) McGuire, J. M.; Powis, P. J. Gas Chromatographic Analysis of Tall Oil Fractionation Products After Methylation with N,N-Dimethylformamide Dimethylacetal. J Chromatogr Sci 1998, 36 (2), 104–108. https://doi.org/10.1093/chromsci/36.2.104.

(15) Landucci, L. L.; Zinkel, D. F. The 1 H and 13 C NMR Spectra of the Abietadienoic Resin Acids. Holzforschung 1991, 45 (5), 341–346. https://doi.org/10.1515/hfsg.1991.45.5.341.0

(16) Yang, G.; Rohde, B. J.; Tesefay, H.; Robertson, M. L. Biorenewable Epoxy Resins Derived from Plant-Based Phenolic Acids. ACS Sustainable Chem. Eng. 2016, 4 (12), 6524–6533. https://doi.org/10.1021/acssuschemeng.6b01343.

(17) Higginson, C. J.; Malollari, K. G.; Xu, Y.; Kelleghan, A. V.; Ricapito, N. G.; Messersmith, P. B. Bioinspired Design Provides High-Strength Benzoxazine Structural Adhesives. Angew. Chem. Int. Ed. 2019, 58 (35), 12271–12279. https://doi.org/10.1002/anie.201906008.

(18) Murawski, A.; Diaz, R.; Inglesby, S.; Delabar, K.; Quirino, R. L. Synthesis of Bio-Based Polymer Composites: Fabrication, Fillers, Properties, and Challenges. In Polymer Nanocomposites in Biomedical Engineering; Sadasivuni, K. K., Ponnamma, D., Rajan, M., Ahmed, B., Al-Maadeed, M. A. S. A., Eds.; Lecture Notes in Bioengineering; Springer International Publishing: Cham, 2019; pp 29–55. https://doi.org/10.1007/978-3-030-04741-2_2.